

---

# Mixture Theories for Rock Properties

James G. Berryman

---

## 1. INTRODUCTION

Two general references for the theory of mixtures are the textbooks of Beran [5] and Christensen [29]. Review articles by Batchelor [3], Hale [41], Hashin [42], Torquato [95], and Willis [110] are also recommended.

### 1.1. Rocks Are Inhomogeneous Materials

A rock is a naturally occurring mixture of minerals. Rocks are normally inhomogeneous both due to their mixed mineral content and due to the presence of cracks and voids. A specimen of a single pure mineral without any cracks or voids is usually called a single crystal, unless the specimen is a jumble of anisotropic and randomly oriented single crystals in which case it is called a polycrystal. When single crystals of different anisotropic minerals are jumbled together randomly, the rock is called a polycrystalline aggregate.

### 1.2. General Assumptions and Caveats

The theory of mixtures as presented here is a macroscopic theory, and assumes that the constituents of the mixture are immiscible (*i.e.*, one component does not dissolve in the presence of another). The theory also assumes at the outset that we know what minerals are contained in a composite (say, using spectroscopic

analysis), what the pertinent physical constants of single crystals of these minerals are (preferably from direct measurements or possibly from independent measurements tabulated in reference books like this one), and usually what the relative volume fractions of these constituents are. In addition, it is sometimes supposed that further information about short-range or long-range order, geometrical arrangements of constituents and pores, or some other pertinent information may be available. Thomsen [93] discusses some of the potential pitfalls involved in using mixture theories to analyze rock data.

We concentrate on three-dimensional results, but wish to point out that two-dimensional results are usually also available and often are somewhat stronger (for example, bounds might be tighter or actually become equalities) than the results quoted here.

When used with real data, all the formulas presented should be analyzed for sensitivity to error propagation from measurement statistics.

The body of knowledge called the theory of mixtures (or the theory of composites) has grown so much in the last 30 years that it is clearly impossible to review all the results pertinent to rocks in a short space. It is the intention of the author to summarize the best established and most generally useful results and then to provide pointers to the literature for more recent and more specialized contributions. Clearly much significant work must be omitted in a review of this size.

---

J. G. Berryman, Lawrence Livermore Laboratory, Earth  
Science, POB 808, L-202, Livermore, CA 94551-9900

Rock Physics and Phase Relations  
A Handbook of Physical Constants  
AGU Reference Shelf 3

sured physical properties. Rigorous bounds are generally based on thermodynamic stability criteria, or on variational principles. For example, the Voigt [98] and Reuss [80] estimates were shown to be rigorous bounds by Hill [46] using variational principles. An estimate is any formula that is neither exact nor a rigorous bound; a truncated series expansion is an example of such an estimate. Derivations of the results are omitted, but may be found in the references.

The significance of these results for rocks differs somewhat from their significance for other types of composite materials used in mechanical design. For example, if one wishes to design a strong but very light weight material (say, for use in structures), bounding methods are clearly superior to estimates: properties of typical elastic composites can be very well approximated when closely spaced bounds are known. However, since rocks virtually always have some porosity, one of the bounds will be practically useless (being either essentially zero or infinity) and, therefore, estimates can play a very significant role in evaluating rock properties.

#### 1.4. Choice of Physical Properties

Results are known for anisotropic composites composed of isotropic constituents and for either isotropic or anisotropic composites of anisotropic constituents. However, to keep this article within bounds, we will say very little about anisotropy. Likewise, frequency dependent results and estimates (or bounds) for complex constants will be largely ignored.

#### 1.5. Format for Presentation of Results

To simplify presentation of results and to emphasize similarities among various estimates and bounds, it will prove convenient to introduce some special notation. Let  $x_1, \dots, x_N$  be the volume fractions of the  $N$  constituents of the composite. We assume that  $x_1 + \dots + x_N = 1$ , so that all the components of the composite are counted. If cracks or voids are present, then the corresponding constituent constants are either zero or infinity (e.g., electrical resistance  $\rho = \infty$  implies a perfect insulator). A volume average of any quantity  $Q(\mathbf{r})$  is given by

$$\langle Q(\mathbf{r}) \rangle = \sum_{i=1}^N x_i Q_i, \quad (1)$$

where  $Q_i$  is the value of  $Q(\mathbf{r})$  in the  $i$ -th component. Reference will be made to the minimum and maximum values  $Q$  takes among all  $N$  constituents, given

by  $Q_{min} = \min_i Q_i$  and  $Q_{max} = \max_i Q_i$ .

To fix notation, we define  $\sigma_{eff}$  as the true effective conductivity,  $\sigma^\pm$  are the upper (+) and lower (-) bounds on conductivity satisfying  $\sigma^- \leq \sigma_{eff} \leq \sigma^+$ , and  $\sigma^*$  is an estimate such that  $\sigma_{eff} \simeq \sigma^*$ . The precise meaning of the expression  $\sigma_{eff} \simeq \sigma^*$  will usually not be specified, but we generally consider only those estimates that are known to satisfy  $\sigma^- \leq \sigma^* \leq \sigma^+$ . The same subscript and superscript notation will be used for all physical properties.

We also introduce certain functions of the constituents' constants [8,11,66,99]. For the conductivity  $\sigma(\mathbf{r})$ , we introduce

$$\begin{aligned} \Sigma(s) &\equiv \left\langle \frac{1}{\sigma(\mathbf{r}) + 2s} \right\rangle^{-1} - 2s \\ &= \left( \sum_{i=1}^N \frac{x_i}{\sigma_i + 2s} \right)^{-1} - 2s. \end{aligned} \quad (2)$$

For the bulk modulus  $K(\mathbf{r})$ , we use

$$\begin{aligned} \Lambda(u) &\equiv \left\langle \frac{1}{K(\mathbf{r}) + \frac{4}{3}u} \right\rangle^{-1} - \frac{4}{3}u \\ &= \left( \sum_{i=1}^N \frac{x_i}{K_i + \frac{4}{3}u} \right)^{-1} - \frac{4}{3}u. \end{aligned} \quad (3)$$

For the shear modulus  $\mu(\mathbf{r})$ , we have

$$\begin{aligned} \Gamma(z) &\equiv \left\langle \frac{1}{\mu(\mathbf{r}) + z} \right\rangle^{-1} - z \\ &= \left( \sum_{i=1}^N \frac{x_i}{\mu_i + z} \right)^{-1} - z. \end{aligned} \quad (4)$$

Each of these three functions increases monotonically as its argument increases. Furthermore, when the argument of each function vanishes, the result is the *harmonic mean* of the corresponding physical property:

$$\begin{aligned} \Sigma(0) &= \left\langle \frac{1}{\sigma(\mathbf{r})} \right\rangle^{-1}, & \Lambda(0) &= \left\langle \frac{1}{K(\mathbf{r})} \right\rangle^{-1}, \\ \text{and} & & \Gamma(0) &= \left\langle \frac{1}{\mu(\mathbf{r})} \right\rangle^{-1}. \end{aligned} \quad (5)$$

Similarly, an analysis of the series expansion for each function at large arguments shows that, in the limit when the arguments go to infinity, the functions approach the *mean* of the corresponding physical property:

$$\begin{aligned} \Sigma(\infty) &= \langle \sigma(\mathbf{r}) \rangle, & \Lambda(\infty) &= \langle K(\mathbf{r}) \rangle, \\ \text{and} & & \Gamma(\infty) &= \langle \mu(\mathbf{r}) \rangle. \end{aligned} \quad (6)$$

Thus, these functions contain both the Reuss [80] and Voigt [98] bounds as limits for positive arguments. Hashin-Shtrikman lower (upper) bounds [44, 45] are obtained by using the minimum (maximum) value of the appropriate constituent property, that is,  $\sigma_{HS}^- = \Sigma(\sigma_{min})$ ,  $\sigma_{HS}^+ = \Sigma(\sigma_{max})$ ,  $K_{HS}^- = \Lambda(\mu_{min})$ ,  $K_{HS}^+ = \Lambda(\mu_{max})$ , etc. Most of the still tighter bounds that are known may be expressed in analogous fashion, but we do not have space to present such results in this review.

Examples, together with comparisons to experiment, are presented to conclude each topic.

## 2. ELECTRICAL CONDUCTIVITY, DIELECTRIC PERMITTIVITY, MAGNETIC PERMEABILITY, THERMAL CONDUCTIVITY, ETC.

The problem of determining the effective electrical conductivity  $\sigma$  of a multiphase conductor is mathematically equivalent to many problems in inhomogeneous materials. Ohm's law relates the current density  $\mathbf{J}$  and the electric field  $\mathbf{E}$  by

$$\mathbf{J} = \sigma \mathbf{E}. \quad (7)$$

In the absence of current sources or sinks, the current density is conserved and therefore satisfies the continuity equation  $\nabla \cdot \mathbf{J} = 0$ . The electric field is the gradient of a potential  $\Phi$ , so  $\mathbf{E} = -\nabla\Phi$ , and is therefore also curl free, so  $\nabla \times \mathbf{E} = 0$ .

For dielectric media, if  $\mathbf{D}$  and  $\mathbf{E}$  are the displacement and electric fields, then the dielectric permittivity  $\epsilon$  satisfies

$$\mathbf{D} = \epsilon \mathbf{E}, \quad (8)$$

where  $\nabla \cdot \mathbf{D} = 0$  in the absence of a charge distribution and  $\nabla \times \mathbf{E} = 0$ .

For magnetic media, if  $\mathbf{B}$  and  $\mathbf{H}$  are the magnetic induction and field intensity, then the magnetic permeability  $\mu$  satisfies

$$\mathbf{B} = \mu \mathbf{H}, \quad (9)$$

where  $\nabla \cdot \mathbf{B} = 0$  and in the absence of currents  $\nabla \times \mathbf{H} = 0$  [52].

For thermal conduction, if  $\mathbf{Q}$  is the heat flux and  $\theta$  is the scalar temperature, then the thermal conductivity  $k$  satisfies

$$\mathbf{Q} = -k \nabla \theta, \quad (10)$$

where heat is conserved according to  $\nabla \cdot \mathbf{Q} = 0$ .

Thus, all of these rather diverse physical problems have the same underlying mathematical structure. We will treat the electrical conductivity as the prototypical problem, although occasionally we use terminology that arose originally in the study of dielectric media.

Historical and technical reviews of the theory of electrical conductivity in inhomogeneous materials are given by Hale [41] and Landauer [59]. Batchelor [3] compares analysis of various transport properties.

### 2.1. Bounds

Hashin-Shtrikman bounds [44, 66] for electrical conductivity may be written using (2)

$$\sigma_{HS}^- \equiv \Sigma(\sigma_{min}) \leq \sigma_{eff} \leq \Sigma(\sigma_{max}) \equiv \sigma_{HS}^+, \quad (11)$$

where we may suppose that the constituents' conductivities have been arranged so that  $\sigma_{min} = \sigma_1 \leq \sigma_2 \leq \dots \leq \sigma_N = \sigma_{max}$ .

Rigorous bounds on the conductivity of polycrystals have been derived by Molyneux [67] and Schulgasser [86].

### 2.2. Estimates

We may use the rigorous bounds to help select useful approximations. Any approximation that violates the bounds may be discarded, since it is not as accurate an estimate as the bounds themselves. We therefore prefer estimates that satisfy (or at worst coincide with) the bounds.

**2.2.1 Spherical inclusions.** One of the earliest estimates of the effective dielectric constant is associated with various names, such as Clausius-Mossotti, Maxwell-Garnett, and Lorentz-Lorenz (see Bergman [6]). The formula for a two-component ( $N = 2$ ) composite with type-2 host containing type-1 spherical inclusions is

$$\begin{aligned} \frac{\epsilon_{CM}^* - \epsilon_2}{\epsilon_{CM}^* + 2\epsilon_2} &= x_1 \frac{\epsilon_1 - \epsilon_2}{\epsilon_1 + 2\epsilon_2} \\ \text{or} \\ \frac{1}{\epsilon_{CM}^* + 2\epsilon_2} &= \left\langle \frac{1}{\epsilon(\mathbf{r}) + 2\epsilon_2} \right\rangle. \end{aligned} \quad (12)$$

Using definition (2), the equivalent result for conductivity is given by

$$\sigma_{CM}^* = \Sigma(\sigma_2). \quad (13)$$

Interchanging the roles of the host and inclusion phases gives a second result  $\sigma_{CM}^* = \Sigma(\sigma_1)$ . Thus, we see that these *estimates* are actually the same as the Hashin-Shtrikman *bounds*.

The self-consistent (SC) effective medium theory for dielectric or conducting composites was derived by Bruggeman [22] and Landauer [58], respectively. Using conductivity as our example, the formula can be written either as

$$\sum_{i=1}^N x_i \frac{\sigma_i - \sigma_{SC}^*}{\sigma_i + 2\sigma_{SC}^*} = 0, \quad (14)$$

or equivalently as

$$\frac{1}{\sigma_{SC}^* + 2\sigma_{SC}^*} = \left\langle \frac{1}{\sigma(x) + 2\sigma_{SC}^*} \right\rangle. \quad (15)$$

Using definition (2), we see that  $\sigma_{SC}^*$  is the fixed point of the function  $\Sigma(\sigma)$  given by

$$\sigma_{SC}^* = \Sigma(\sigma_{SC}^*). \quad (16)$$

This equation makes it clear that the solution is found through iteration, and that is one reason the method is called “self-consistent.”

The differential (D) effective medium approach was first proposed by Bruggeman [22]. If there are only two constituents whose volume fractions are  $x = v_1$  and  $y = v_2 = 1-x$  with type-1 material being the host and type-2 being inclusion, then suppose the value of the effective conductivity  $\sigma_D^*(y)$  is known for the value  $y$ . Treating  $\sigma_D^*(y)$  as the host conductivity and  $\sigma_D^*(y+dy)$  as that of the infinitesimally altered composite, we find

$$(1-y) \frac{d}{dy} [\sigma_D^*(y)] = \frac{\sigma_2 - \sigma_D^*(y)}{\sigma_2 + 2\sigma_D^*(y)} [3\sigma_D^*(y)]. \quad (17)$$

This equation can be integrated analytically. Starting with  $\sigma_D^*(0) = \sigma_1$ , we find

$$\left( \frac{\sigma_2 - \sigma_D^*(y)}{\sigma_2 - \sigma_1} \right) \left( \frac{\sigma_1}{\sigma_D^*(y)} \right)^{\frac{1}{3}} = 1 - y. \quad (18)$$

Milton [65] has shown that the self-consistent effective medium method produces results that are realizable and therefore always satisfy the rigorous bounds. Norris *et al.* [71] have shown the corresponding result for the differential effective medium theory.

**2.2.2. Nonspherical inclusions.** When considering nonspherical inclusions (generally assumed to be ellipsoidal), it is convenient to introduce the factors  $R$  defined by

$$R^{mi} = \frac{1}{9} \sum_{p=a,b,c} \frac{1}{L_p \sigma_i + (1-L_p) \sigma_m} \quad (19)$$

(examples are displayed in Table 1). The superscripts  $m$  and  $i$  refer to matrix (host) and inclusion phases, while the  $L_p$ s are the depolarization factors along each of the principle directions ( $a, b, c$ ) of an ellipsoidal inclusion. A generalization of the Clausius-Mossotti formula for nonspherical inclusions in an isotropic composite is (see Cohen *et al.* [32] and Galeener [39])

$$\frac{\sigma_{CM}^* - \sigma_m}{\sigma_{CM}^* + 2\sigma_m} = \sum_{i=1}^N x_i (\sigma_i - \sigma_m) R^{mi}. \quad (20)$$

A generalization of the self-consistent formula for nonspherical inclusions in an isotropic composite is

$$\sum_{i=1}^N x_i (\sigma_i - \sigma_{SC}^*) R^{*i} = 0. \quad (21)$$

The asterisk superscript for  $R$  simply means that the host material has the conductivity  $\sigma_{SC}^*$ . Thus, (20) is explicit, while (21) is implicit.

Tabulations of the depolarizing factors  $L_p$  for general ellipsoids are given by Osborn [72] and Stoner [91].

For aligned ellipsoids (*i.e.*, for certain anisotropic conductors), if the depolarization factor of the axis aligned with the applied field is  $L$ , then Sen *et al.* [88] show that the differential effective medium estimate can again be integrated analytically and produces the result

$$\left( \frac{\sigma_2 - \sigma_D^*(y)}{\sigma_2 - \sigma_1} \right) \left( \frac{\sigma_1}{\sigma_D^*(y)} \right)^L = 1 - y. \quad (22)$$

TABLE 1. Three examples of coefficients  $R$  for spherical and nonspherical inclusions in isotropic composites. The superscripts  $m$  and  $i$  refer to matrix (host) and inclusion phases, respectively.

Inclusion shape	Depolarizing factors $L_a, L_b, L_c$	$R^{mi}$
Spheres	$\frac{1}{3}, \frac{1}{3}, \frac{1}{3}$	$\frac{1}{\sigma_i + 2\sigma_m}$
Needles	$0, \frac{1}{2}, \frac{1}{2}$	$\frac{1}{9} \left( \frac{1}{\sigma_m} + \frac{4}{\sigma_i + \sigma_m} \right)$
Disks	$1, 0, 0$	$\frac{1}{9} \left( \frac{1}{\sigma_i} + \frac{2}{\sigma_m} \right)$

The result (18) is seen to be a special case of this more general result with  $L = \frac{1}{3}$ .

A paper by Stroud [92] introduced a self-consistent effective medium theory for conductivity of polycrystals.

**2.2.3. Series expansion methods.** Brown [21] has shown how to obtain estimates of conductivity using series expansion methods.

### 2.3. Example

**2.3.1. Formation factor of glass-bead packings.** The formation factor  $F$  for a porous medium is defined as

$$F = \sigma / \sigma^*, \quad (23)$$

where  $\sigma$  is the electrical conductivity of the pore fluid and  $\sigma^*$  is the overall conductivity of the saturated porous medium -- assuming that the material composing the porous frame is nonconducting. A related quantity called the electrical tortuosity  $\tau$  is determined by the formula

$$\tau = \phi F. \quad (24)$$

Johnson *et al.* [54] have measured the electrical conductivity of a series of glass-bead packings with conducting fluid saturating the porosity  $\phi$ . The corresponding values of  $F$  are shown in Figure 1 and Table

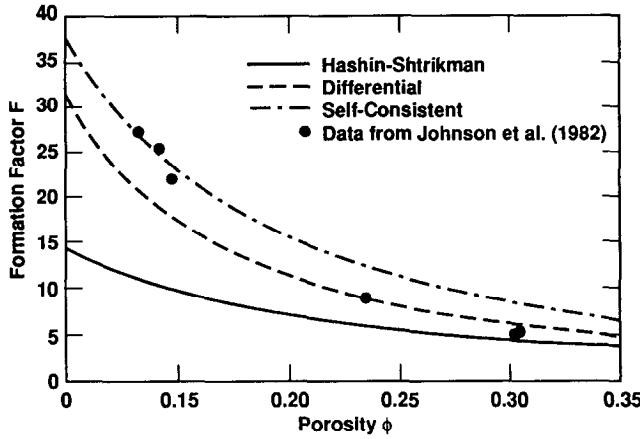


Fig. 1. Measurements of formation factor  $F$  compared to Hashin-Shtrikman bounds and estimates based on the differential (D) scheme for spherical insulating particles in a conducting fluid and the self-consistent (SC) method for spherical insulators and needle-shaped conductors. Data from Johnson *et al.* [54].

TABLE 2. Comparison of measured and calculated formation factor  $F$  for packings of glass beads. Data from Johnson *et al.* [54].

Porosity	Experimental	Spheres	Spheres-Needles
$\phi$	$F$	$F_D$	$F_{SC}$
0.133	27.2	20.6	26.6
0.142	25.4	18.7	24.5
0.148	22.0	17.6	23.2
0.235	8.8	8.8	12.3
0.303	5.0	6.0	8.2
0.305	5.2	5.9	8.1

2. All the values lie above the Hashin-Shtrikman lower bound on  $F$ , given by

$$F_{HS}^- = 1 + \frac{3}{2} \frac{1 - \phi}{\phi}, \quad (25)$$

as expected.

The paper by Sen *et al.* [88] shows that the differential (D) method predicts the formation factor should be given by

$$F_D = \phi^{-\frac{3}{2}}, \quad (26)$$

assuming that the glass beads are treated as nonconducting spheres imbedded in a host medium corresponding to the conducting fluid. This approach guarantees that the conducting fluid contains connected (and therefore conducting) pathways at all values of the porosity.

The self-consistent (SC) method can also be used by assuming the glass beads are spheres in the conducting fluid in the very high porosity limit and that the porosity is in the form of needle-shaped voids in the glass in the low porosity limit. The resulting formula is given by

$$F_{SC} = \frac{1}{2} (X - 1 + [(X + 1)^2 + 32])^{\frac{1}{2}}, \quad (27)$$

where

$$X = -3 + \frac{9}{2} \frac{1 - \phi}{\phi}. \quad (28)$$

(If the sphere-sphere version of the SC approximation had been used instead, we would have found that the SC method predicts there are no conducting paths through the sample for porosities  $\phi \leq \frac{1}{3}$ . However, this result just shows that a spherical geometry for the

TABLE 3. Conversion formulas for the various elastic constants.

<i>Bulk modulus</i>	<i>Shear modulus</i>	<i>Young's modulus</i>	<i>Poisson's ratio</i>
$K$	$\mu$	$E$	$\nu$
$K = \frac{E}{3(1-2\nu)}$	$\mu = \frac{E}{2(1+\nu)}$	$\frac{1}{E} = \frac{1}{9K} + \frac{1}{3\mu}$	$\nu = \frac{3K-2\mu}{2(3K+\mu)}$

pores is an inadequate representation of the true microstructure at low porosities. That is why we choose needles instead to approximate the pore microstructure.)

These two theoretical estimates are also listed and shown for comparison in Table 2 and Figure 1. We find that the differential method agrees best with the data at the higher porosities ( $\simeq 25\text{-}30\%$ ), while the self-consistent effective medium theory agrees best at the lower porosities ( $\simeq 15\%$ ). These results seem to show that needle-shaped pores give a reasonable approximation to the actual pore shapes at low porosity, while such an approximation is inadequate at the higher porosities.

### 3. ELASTIC CONSTANTS

For isotropic elastic media, the bulk modulus  $K$  is related to the Lamé parameters  $\lambda, \mu$  of elasticity [see Eq. (54)] by

$$K = \lambda + \frac{2}{3}\mu, \quad (29)$$

where  $\mu$  is the shear modulus. Bounds and estimates are normally presented in terms of the bulk and shear moduli. However, results of mechanical measurements are often expressed (particularly in the engineering literature) in terms of Young's modulus  $E$  and Poisson's ratio  $\nu$ . Useful relations among these constants are displayed for ease of reference in Table 3.

A very useful review article on the theory of elastic constants for inhomogeneous media and applications to rocks is that of Watt *et al.* [108]. The textbook by Christensen [29] may also be highly recommended. Elastic anisotropy due to fine layering has been treated by Backus [2].

#### 3.1. Exact

When all the constituents of an elastic composite have the same shear modulus  $\mu$ , Hill [47] has shown

that the effective bulk modulus  $K_{eff}$  is given by the exact formula

$$\frac{1}{K_{eff} + \frac{4}{3}\mu} = \left\langle \frac{1}{K(\mathbf{x}) + \frac{4}{3}\mu} \right\rangle, \quad (30)$$

or equivalently

$$K_{eff} = \Lambda(\mu), \quad (31)$$

using the function defined in (3). Clearly,  $\mu_{eff} = \mu$  if the shear modulus is constant.

If all constituents are fluids, then the shear modulus is constant and equal to zero. Thus, Hill's result (30) shows that the bulk modulus of a fluid mixture is just the Reuss average or harmonic mean of the constituents' moduli. This fact is the basis of Wood's formula [see (48)] for wave speeds in fluid/fluid mixtures and fluid/solid suspensions.

#### 3.2. Bounds

Hashin-Shtrikman [43] bounds for the bulk modulus are

$$K_{HS}^- \equiv \Lambda(\mu_{min}) \leq K_{eff} \leq \Lambda(\mu_{max}) \equiv K_{HS}^+. \quad (32)$$

For the shear modulus, we first define the function

$$\zeta(K, \mu) = \frac{\mu}{6} \left( \frac{9K+8\mu}{K+2\mu} \right). \quad (33)$$

Note that  $\zeta(K, \mu)$  is a monotonically increasing function of its arguments whenever they are both positive. When the constituents' elastic moduli are well-ordered so that  $K_{min} = K_1 \leq \dots \leq K_N = K_{max}$  and  $\mu_{min} = \mu_1 \leq \dots \leq \mu_N = \mu_{max}$ , then the Hashin-Shtrikman bounds for the shear modulus are

$$\begin{aligned} \mu_{HS}^- &\equiv \Gamma(\zeta(K_{min}, \mu_{min})) \leq \mu_{eff} \\ &\leq \Gamma(\zeta(K_{max}, \mu_{max})) \equiv \mu_{HS}^+, \end{aligned} \quad (34)$$

using (33). When the constituents' properties are not

well-ordered, we may still number the components so that  $K_{min} = K_1 \leq \dots \leq K_N = K_{max}$ , but now  $\mu_{min} \equiv \min_{i=1,N} \mu_i$  and  $\mu_{max} \equiv \max_{i=1,N} \mu_i$ . Then, the bounds in (34) are still valid (with the different definitions of  $\mu_{min}$  and  $\mu_{max}$ ), but they are usually called either the Walpole bounds [99] or the Hashin-Shtrikman-Walpole bounds.

Since experimental data are very often presented in terms of  $E$  and  $\nu$  — Young's modulus and Poisson's ratio, respectively — we should consider the transformation from the  $(K, \mu)$ -plane to the  $(E, \nu)$ -plane (see Figure 2) and its impact on the corresponding bounds. The Hashin-Shtrikman bounds define a rectangle in  $(K, \mu)$  with the corners given by the points  $(K^-, \mu^-)$ ,  $(K^+, \mu^-)$ ,  $(K^+, \mu^+)$ , and  $(K^-, \mu^+)$ . Each of these corners corresponds to a distinct limiting value of either  $E$  or  $\nu$ . For example, since Young's modulus is determined from the expression

$$\frac{1}{E} = \frac{1}{9K} + \frac{1}{3\mu}, \quad (35)$$

we see that  $E$  is a monotonically increasing function of both  $K$  and  $\mu$ . Thus, the diagonal corners  $(K^-, \mu^-)$  and  $(K^+, \mu^+)$  of the Hashin-Shtrikman rectangle determine the lower and upper HS bounds ( $E_{HS}^-$  and  $E_{HS}^+$ ) on Young's modulus. Similarly, since

$$\mu = \frac{3(1-2\nu)}{2(1+\nu)} K, \quad (36)$$

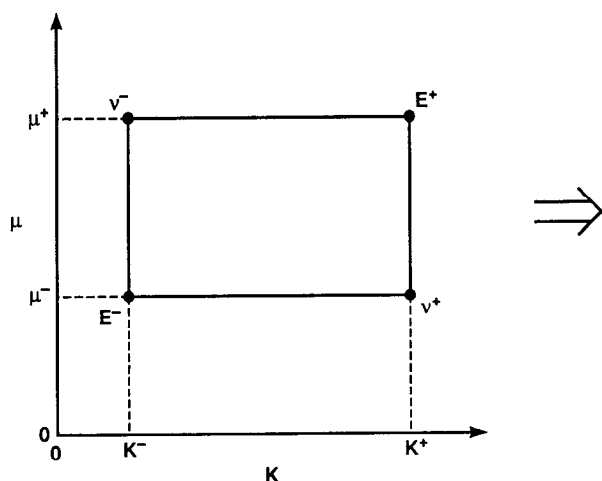
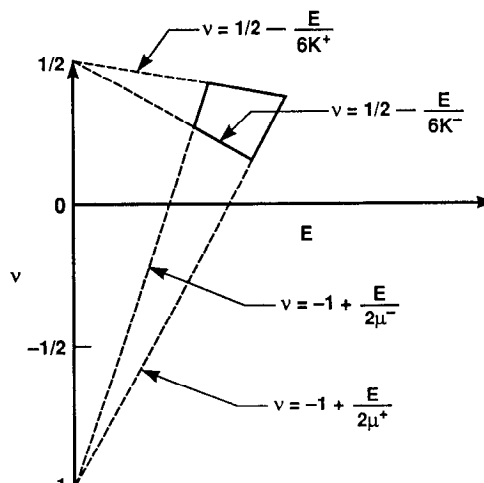


Fig. 2. Schematic illustration of the transformation of a Hashin-Shtrikman rectangle for  $(K, \mu)$ -bounds to a quadrilateral for  $(E, \nu)$ -bounds. Corners of the  $(K, \mu)$  rectangle correspond to the bounding values in  $(E, \nu)$ .

and since the coefficient of  $K$  in (36) is a monotonically decreasing function of  $\nu$  for all physical values in the range  $(-1, 1/2)$ , we find easily that minimum and maximum values of Poisson's ratio  $\nu_{HS}^-$  and  $\nu_{HS}^+$  occur respectively at the corners  $(K^-, \mu^+)$  and  $(K^+, \mu^-)$ . Although these bounds are rigorous, better bounds in the  $(E, \nu)$ -plane are given by the solid outlines of the quadrilateral region shown in Figure 2; the full range of possible pairs  $(E, \nu)$ , as determined by the Hashin-Shtrikman bounds [116], lies within this quadrilateral. The displayed equations for the four dotted lines shown in Figure 2 follow easily from the relations in Table 3.

If the composite contains porosity, then the lower Hashin-Shtrikman bounds on the bulk and shear moduli become trivial (zero), so the Hashin-Shtrikman rectangle is bounded by the  $K$  and  $\mu$  axes. Similarly, when transformed into the  $(E, \nu)$ -plane, we find that the only nontrivial universal bound remaining is  $E_{HS}^+$ , since the overall bounds on Poisson's ratio are the same as the physical limits  $\nu_{HS}^- = -1$  and  $\nu_{HS}^+ = 1/2$ . The full range of possible pairs  $(E, \nu)$  is now determined by the triangular region shown in Figure 3. In some of our tables, the value  $\nu(K_{HS}^+, \mu_{HS}^+)$  is listed — not because it is a bound (it is not) — but because it is the value of  $\nu$  corresponding to the point of highest possible  $E = E_{HS}^+$ .

Finally, note that data are also sometimes presented in terms of  $(E, \mu)$  pairs. The preceding results



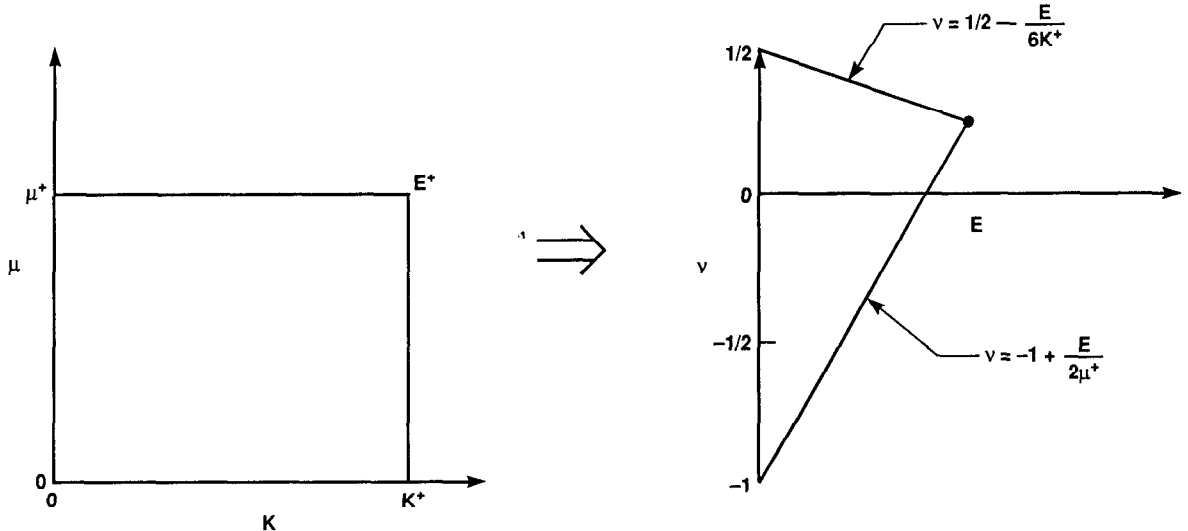


Fig. 3. Schematic as in Fig. 2, but for porous materials where  $K_{HS}^- = 0 = \mu_{HS}^-$ . Hashin-Shtrikman rectangles in  $(K, \mu)$  become triangles in  $(E, \nu)$ .

show that the HS rectangle in the  $(K, \mu)$ -plane then transforms to another rectangle in the  $(E, \mu)$ -plane.

Hashin and Shtrikman [45] also derived variational bounds for the effective moduli of polycrystals of materials with cubic symmetry. Peselnick and Meister [76] derived bounds like those of Hashin and Shtrikman for the effective moduli of polycrystals composed of materials with hexagonal and trigonal symmetries. Walpole [100] provides an elegant derivation of these bounds for polycrystals. Simmons and Wang [89] tabulate single crystal data and also the bounds for polycrystals of many cubic minerals. Watt [107] has reviewed the literature on applications of Hashin-Shtrikman bounds to polycrystals and found very good agreement between the bounds and data when experimental errors in the data are taken into account.

### 3.3. Estimates

Since rigorous bounds are known, it is preferable to consider estimates that always satisfy (or are at least no worse than) the bounds.

**3.3.1. Voigt-Reuss-Hill.** Hill [46] has shown that the Voigt and Reuss averages are upper and lower bounds on the moduli. A common approximation (see Chung [30], Peselnick [75], Peselnick and Meister [76], and Thomsen [93]) based on these bounds is the Voigt-Reuss-Hill estimate obtained by taking the arithmetic mean of the bounds. Brace [18] made extensive use of this estimate and found that for low porosity rocks at high pressure the agreement with experiment was excellent.

**3.3.2. Spherical inclusions.** A review of the derivation of various single-scattering approximations in elasticity is contained in Berryman [9].

Kuster and Toksöz [55] derive estimates of bulk and shear moduli of composites within a single-scattering approximation assuming that one of the constituents (say type-1) serves as the host medium. For spherical scatterers,

$$K_{KT}^* = \Lambda(\mu_1) \quad \text{and} \quad \mu_{KT}^* = \Gamma(\zeta(K_1, \mu_1)), \quad (37)$$

where  $\zeta(K, \mu)$  was defined in (33). These formulas have the advantage of being explicit (*i.e.*, requiring neither iteration nor integration). There are also as many estimates as constituents, since any constituent desired may be chosen as the host. If the host medium is either the stiffer or the most compliant, then these formulas produce the same values as the corresponding Hashin-Shtrikman bounds.

For inclusions that are spherical in shape, the self-consistent effective medium estimates [7, 23, 48, 101] for the bulk and shear moduli are

$$K_{SC}^* = \Lambda(\mu_{SC}^*) \quad \text{and} \quad \mu_{SC}^* = \Gamma(\zeta(K_{SC}^*, \mu_{SC}^*)), \quad (38)$$

where  $\zeta(K, \mu)$  was defined in (33). These values are found by iterating to the fixed point which is known to be stable and unique for positive values of the moduli. This estimate is completely symmetric in all the constituents, so no single component plays the role of host for the others.

TABLE 4. Four examples of coefficients  $P$  and  $Q$  for spherical and nonspherical scatterers. The superscripts  $m$  and  $i$  refer to matrix (host) and inclusion phases, respectively. Special characters are defined by  $\beta = \mu[(3K + \mu)/(3K + 4\mu)]$ ,  $\gamma = \mu[(3K + \mu)/(3K + 7\mu)]$ , and  $\zeta = (\mu/6)[(9K + 8\mu)/(K + 2\mu)]$ . The expression for spheres, needles, and disks were derived by Wu [112] and Walpole [101]. The expressions for penny-shaped cracks were derived by Walsh [102] and assume  $K_i/K_m \ll 1$  and  $\mu_i/\mu_m \ll 1$ . The aspect ratio of the cracks is  $\alpha$ .

Inclusion shape	$P^{mi}$	$Q^{mi}$
Spheres	$\frac{K_m + \frac{4}{3}\mu_m}{K_i + \frac{4}{3}\mu_m}$	$\frac{\mu_m + \zeta_m}{\mu_i + \zeta_m}$
Needles	$\frac{K_m + \mu_m + \frac{1}{3}\mu_i}{K_i + \mu_m + \frac{1}{3}\mu_i}$	$\frac{1}{5} \left( \frac{4\mu_m}{\mu_m + \mu_i} + 2\frac{\mu_m + \gamma_m}{\mu_i + \gamma_m} + \frac{K_i + \frac{4}{3}\mu_m}{K_i + \mu_m + \frac{1}{3}\mu_i} \right)$
Disks	$\frac{K_m + \frac{4}{3}\mu_i}{K_i + \frac{4}{3}\mu_i}$	$\frac{\mu_m + \zeta_i}{\mu_i + \zeta_i}$
Penny cracks	$\frac{K_m + \frac{4}{3}\mu_i}{K_i + \frac{4}{3}\mu_i + \pi\alpha\beta_m}$	$\frac{1}{5} \left( 1 + \frac{8\mu_m}{4\mu_i + \pi\alpha(\mu_m + 2\beta_m)} + 2\frac{K_i + \frac{2}{3}(\mu_i + \mu_m)}{K_i + \frac{4}{3}\mu_i + \pi\alpha\beta_m} \right)$

The differential effective medium approach [31] applies an idea of Bruggeman [22] to the elastic constant problem. If there are only two constituents whose volumes fractions are  $x = v_1$  and  $y = v_2 = 1 - x$  with the type-1 material being host and type-2 being inclusion, then suppose the value of the effective bulk modulus  $K_D^*(y)$  is known for the value  $y$ . Treating the  $K_D^*(y)$  as the bulk modulus of the host medium and  $K_D^*(y + dy)$  as the modulus of the composite, we find

$$(1 - y) \frac{d}{dy} [K_D^*(y)] = \frac{K_2 - K_D^*(y)}{K_2 + \frac{4}{3}\mu_D^*(y)} \times \\ \left[ K_D^*(y) + \frac{4}{3}\mu_D^*(y) \right] \quad (39)$$

and similarly

$$(1 - y) \frac{d}{dy} [\mu_D^*(y)] = \frac{\mu_2 - \mu_D^*(y)}{\mu_2 + \zeta(K_D^*(y), \mu_D^*(y))} \times \\ [\mu_D^*(y) + \zeta(K_D^*(y), \mu_D^*(y))], \quad (40)$$

where  $\zeta$  was defined in (33). Note that (39) and (40) are coupled and therefore must be integrated simultaneously. Unlike the self-consistent effective medium results quoted in the preceding paragraph, the differential effective medium approach is not symmetric in the components and therefore produces two different estimates depending on which constituent plays the role of host and which the inclusion phase.

**3.3.3. Nonspherical inclusions.** In the presence of nonspherical inclusions, the Kuster-Toksöz and self-consistent effective medium methods can both be easily generalized [7, 55].

Using the symbols  $P$  and  $Q$  defined in Table 4, the formulas for the general Kuster-Toksöz approach are

$$(K_{KT}^* - K_m) \frac{K_m + \frac{4}{3}\mu_m}{K_{KT}^* + \frac{4}{3}\mu_m} = \\ \sum_{i=1}^N x_i (K_i - K_m) P^{mi} \quad (41)$$

for the bulk modulus, and

$$(\mu_{KT}^* - \mu_m) \frac{\mu_m + \zeta_m}{\mu_{KT}^* + \zeta_m} = \\ \sum_{i=1}^N x_i (\mu_i - \mu_m) Q^{mi} \quad (42)$$

for the shear modulus. Formulas (41) and (42) are clearly uncoupled and can be rearranged to show they are also explicit, i.e., requiring neither iteration nor integration for their solution.

Similarly, the formulas for the self-consistent effective medium approximations are

$$\sum_{i=1}^N x_i (K_i - K_{SC}^*) P^{*i} = 0 \quad (43)$$

for the bulk modulus, and

$$\sum_{i=1}^N x_i (\mu_i - \mu_{SC}^*) Q^{*i} = 0 \quad (44)$$

for the shear modulus. The asterisk superscript for  $P$  and  $Q$  simply means that the host material has the

TABLE 5. Values of isothermal bulk moduli of porous P-311 glass measured at room temperature compared to theoretical estimates. Bulk and shear moduli of the pure glass were measured to be  $K = 46.3$  and  $\mu = 30.5$  GPa, respectively. All data from Walsh *et al.* [104].

Porosity $\phi$	Experimental	Hashin-Shtrikman	Spherical Voids	Needles-Spheres
	$K$ (GPa)	$K_{HS}^+$ (GPa)	$K_D$ (GPa)	$K_{SC}$ (GPa)
0.00	46.1	46.3	46.3	46.3
0.00	45.9	46.3	46.3	46.3
0.05	41.3	41.6	41.5	41.4
0.11	36.2	36.6	36.1	35.6
0.13	37.0	35.1	34.4	33.7
0.25	23.8	27.0	25.2	22.8
0.33	21.0	22.5	19.9	16.4
0.36	18.6	21.0	18.1	14.2
0.39	17.9	19.6	16.4	12.3
0.44	15.2	17.3	13.7	9.4
0.46	13.5	15.5	12.7	8.5
0.50	12.0	14.8	10.9	6.7
0.70	6.7	7.7	3.8	2.1

moduli  $K_{SC}^*$  and  $\mu_{SC}^*$ . The solutions to (43) and (44) are found by simultaneous iteration.

Based on earlier work by Eshelby [35] for ellipsoidal inclusions, Wu [112], Kuster and Toksöz [55], and Berryman [7] give general expressions for  $P^{mi}$  and  $Q^{mi}$  for spheroidal inclusions.

**3.3.4. Series expansion methods.** Beran [5] and Molyneux and Beran [68] have used series expansion methods to obtain estimates of the elastic constants.

#### 3.4. Examples

**3.4.1. Porous glass.** Walsh *et al.* [104] made measurements on the compressibility ( $1/K$ ) of a porous glass over a wide range of porosities. The samples they used were fabricated from P-311 glass powder. The powder and binder were die-pressed and then sintered. Depending on the thermal history of the samples, they obtained a porous glass foam with porosities ranging from 0.70 to near zero. Porosity measurements were stated to be accurate  $\pm 0.01$ . Linear compressibility of the samples was measured. Their results agreed well with the theoretical predictions of Mackenzie [63]. It

turns out that Mackenzie's result for the bulk modulus of a porous solid is also identical to the upper Hashin-Shtrikman bound for this problem. Thus, Walsh *et al.* [104] actually showed that their porous glass satisfies the HS bounds for a wide range of porosities and, furthermore, that the values they found closely track the upper bound.

Results of the theoretical calculations are shown in Table 5 and Figure 4. To be consistent with the microgeometry of these porous glasses for the SC approximation, we have treated the glass as if it were shaped like needles randomly dispersed in the void at the highest porosities; the voids are treated as spherical inclusions in the glass at the lowest porosities. (If instead we had chosen to treat the glass as spheres, the SC approximation would have vanished at porosities of 50 % and greater. However, spheres of glass serve as a very unrealistic representation of the true microstructure of the porous medium at high porosities.) Since the differential approximation treats the glass as host medium at all values of porosity, we need assume only that the voids are spherical for this estimate. We see that both theories (SC and D) do well at predicting

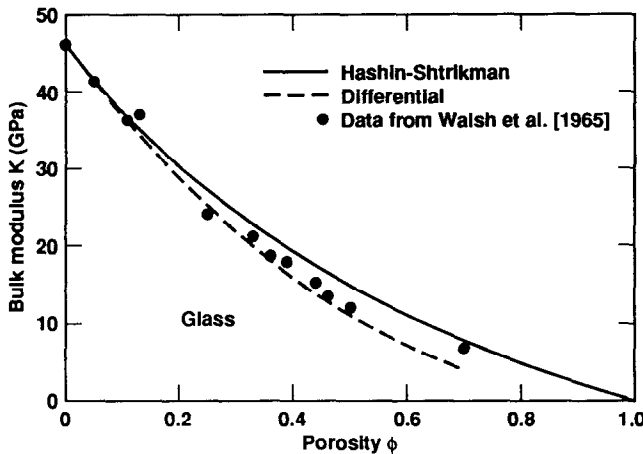


Fig. 4. Isothermal bulk modulus  $K$  of porous P-311 glass measured at room temperature compared to the Hashin-Shtrikman upper bound (solid line) and differential (D) scheme (dashed line) assuming spherical voids. Data from Walsh *et al.* [104].

the measured values out to about 25% porosity. For higher porosities, both theories overestimate the influence of the voids while the Hashin-Shtrikman bound (equivalent to the KT theory for this problem) does somewhat better at estimating the measured values over the whole range of porosities. Also see Zimmerman [115].

**3.4.2. Porous silicon nitride.** Fate [36] has performed a series of experiments measuring elastic constants of polycrystalline silicon nitride ( $Si_3N_4$ ). The elastic constant data are believed to be accurate to  $\pm 3\%$ , but errors may be somewhat larger for the lowest density samples. The data are shown in Table 6 and Figure 5. Fate showed approximate agreement with Budiansky's theory [23] in the original paper, but, for this problem, Budiansky's theory is just the same as our SC approximation for spherical inclusions. For comparison, the SC estimates for spherical particles and needle-shaped pores are also listed in the Table. The overall agreement with the data is improved somewhat using this estimate. The differential estimate for spherical inclusions was also computed (but is not shown here) and again found to overestimate the importance of the voids in the overall properties of the composite for porosities greater than 15 %.

There is one anomaly in this data set at  $\phi = 0.025$ . The measured value of  $E$  is larger than the value for the sample at  $\phi = 0.0$ , suggesting either that the true value of Young's modulus for the nonporous sample

has been underestimated, or that the actual value of the porosity for that sample was overestimated. See the data of Fisher *et al.* [37] and Fisher *et al.* [38].

#### 4. ACOUSTIC AND SEISMIC VELOCITIES

In isotropic elastic solids, the compressional wave speed  $V_c$  is related to the elastic constants and density  $\rho$  by

$$V_c = \left( \frac{K + \frac{4}{3}\mu}{\rho} \right)^{\frac{1}{2}} \quad (45)$$

and the shear wave speed  $V_s$  is given by

$$V_s = \left( \frac{\mu}{\rho} \right)^{\frac{1}{2}}. \quad (46)$$

In a pure fluid, the shear modulus is negligible so no shear wave appears and the acoustic velocity  $V_f$  is

$$V_f = \left( \frac{K_f}{\rho_f} \right)^{\frac{1}{2}}. \quad (47)$$

Reviews of mixture theory for wave propagation are given in Hudson [51] and Willis [110], and also in the reprint volume edited by Wang and Nur [106].

##### 4.1. Exact

In a fluid mixture or a fluid suspension (solid inclusions completely surrounded by fluid), Wood's formula [111] for sound velocity is determined by using the bulk modulus of a suspension (the harmonic mean) and the average density, so

$$V_{Wood} = \left( \frac{K_{eff}}{\rho_{eff}} \right)^{\frac{1}{2}}, \quad (48)$$

where

$$\frac{1}{K_{eff}} = \frac{x_f}{K_f} + \sum_{i=1}^{N-1} \frac{x_i}{K_i} \quad (49)$$

and

$$\rho_{eff} = x_f \rho_f + \sum_{i=1}^{N-1} x_i \rho_i. \quad (50)$$

This result is essentially exact for low frequencies (*i.e.*, when the wavelength is long compared to the size of the inclusions), since (49) [also see (31)] is the exact effective bulk modulus for quasistatic deformations. How-

TABLE 6. Values of adiabatic elastic moduli of porous polycrystalline silicon nitride measured at room temperature compared to theoretical estimates. Young's modulus and the shear modulus of the pure  $Si_3N_4$  were measured to be  $E = 289.0$  and  $\mu = 118.2$  GPa, respectively. All data from Fate [36].

<i>Porosity</i>	<i>Experimental</i>	<i>Hashin-Shtrikman</i>	<i>Sphere-Sphere</i>	<i>Sphere-Needle</i>
$\phi$	$E$ (GPa)	$E_{HS}^+$ (GPa)	$E_{SC}$ (GPa)	$E_{SC}$ (GPa)
0.000	289.0	289.0	289.0	289.0
0.025	292.1	274.9	274.4	272.2
0.028	259.3	273.1	272.7	270.2
0.041	244.4	266.2	265.3	261.5
0.151	172.3	213.1	201.6	189.3
0.214	142.9	187.0	165.1	149.3
0.226	131.8	182.4	158.2	141.7
0.255	128.2	171.3	141.5	123.6
$\phi$	$\mu$ (GPa)	$\mu_{HS}^+$ (GPa)	$\mu_{SC}$ (GPa)	$\mu_{SC}$ (GPa)
0.000	118.2	118.2	118.2	118.2
0.025	117.6	112.5	112.3	111.4
0.028	111.0	111.8	111.6	110.6
0.041	100.7	109.0	108.6	107.1
0.151	72.4	87.4	82.8	77.8
0.214	61.1	76.8	67.9	61.5
0.226	53.4	74.9	65.1	58.4
0.255	54.8	70.4	58.3	51.0

ever, care should be taken to use the adiabatic (as opposed to the isothermal) moduli in (49). Although the difference between adiabatic and isothermal moduli is generally small for solids, it may be significant for fluids.

#### 4.2. Bounds

Bounds on wave speed may be obtained using Fermat's principle of least traveltime. Since Fermat's principle states that traveltime  $T_{AB}$  along a ray path from point  $A$  to point  $B$  is given by

$$T_{AB} = \min_{\{paths\}} \int \frac{1}{V(\mathbf{x})} dl, \quad (51)$$

where  $dl$  is the infinitesimal increment along the ray path. Then, if the straight-line distance between  $A$

and  $B$  is  $L_{AB}$ , the effective wave speed is related to constituent wave speeds by

$$\frac{1}{V_{eff}} \equiv \frac{T_{AB}}{L_{AB}} \leq \frac{x_f}{V_f} + \sum_{i=1}^{N-1} \frac{x_i}{V_i} \equiv \frac{1}{V_{Wyllie}}, \quad (52)$$

where  $V_f$  is the wave speed of the primary fluid and the  $V_i$ s are the compressional wave speeds of the other constituents, while  $x_f$  and  $x_i$  are the corresponding volume fractions. The inequality in (52) is based on the assumption that any macroscopic straight line of length  $L_{AB}$  in a random medium will have lengths  $\sum x_i L_{AB}$  passing through solid and  $x_f L_{AB}$  passing through fluid. An actual ray path will not be straight however (due to refraction), so the true traveltime will be less than that predicted by the average slowness

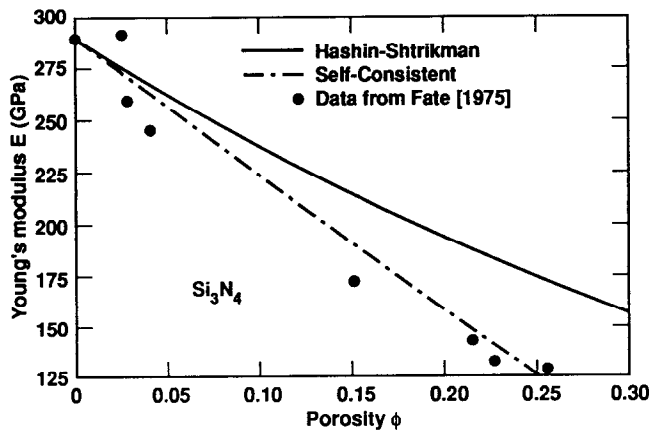


Fig. 5a. Young's modulus  $E$  of porous silicon nitride ( $\text{Si}_3\text{N}_4$ ). Hashin-Shtrikman upper bound is the solid line. The self-consistent (SC) estimate assuming spherical particles and needle-shaped pores is the dot-dash line. Data from Fate [36].

on the right of (52) known as Wyllie's time average formula [113,114]. Since Wyllie *et al.*'s estimate of the sound speed in a mixture is based in part on Fermat's principle, it should be viewed as a lower bound not as an estimate.

#### 4.3. Estimates

Estimates of the wave velocities are usually based on the corresponding estimates of the bulk and shear moduli, such as those discussed in Section 3.3.

#### 4.4. Examples

Constituent properties required for the three examples are listed in Table 7.

**4.4.1. Liquid/gas mixture.** Wood's formula is known to apply to a liquid/gas mixture. Considering air in water, we have  $K_{\text{air}} = 1.2 \times 10^{-4}$  GPa,  $\rho_{\text{air}} = 0.0012$  g/cc,  $K_{\text{water}} = 2.25$  GPa,  $\rho_{\text{water}} = 1.00$  g/cc. Figure 6 shows the result of the calculation.

Wyllie's formula should not be applied to mixtures containing gas.

**4.4.2. Liquid/liquid mixture.** Wang and Nur [105] obtained ultrasonic velocity data for pure hydrocarbons and mixtures. Although the hydrocarbons are miscible and, therefore, violate the usual immiscibility assumption of mixture theories, we still expect that these data may be properly analyzed using Wood's formula and Wyllie's time average equation. The mea-

sured velocities and densities for the pure alkenes used in the mixture are presented in Table 7 along with the computed adiabatic bulk moduli. This information is used in Table 8 and Figure 7 to show that the two formulas agree with the data to within 1%. Also note the general relationship between  $V_{\text{Wood}}$  and  $V_{\text{Wyllie}}$  illustrated here that

$$\left[ \sum x_i \rho_i \sum \frac{x_i}{K_i} \right]^{-\frac{1}{2}} = V_{\text{Wood}}$$

$$\leq V_{\text{Wyllie}} = \left[ \sum x_i \left( \frac{\rho_i}{K_i} \right)^{\frac{1}{2}} \right]^{-1}, \quad (53)$$

which is valid for all fluid/fluid mixtures. (Wood's formula is only correct for fluid mixtures and suspensions, whereas Wyllie's formula applies to arbitrary liquid/liquid and solid/liquid mixtures. Thus, the inequality (53) is of interest for liquid/liquid mixtures). Inequality (53) follows from Cauchy's inequality for sums:  $(\sum a_i b_i)^2 \leq \sum a_i^2 \sum b_i^2$ .

**4.4.3. Liquid/solid suspensions.** Kuster and Toksöz [56] performed ultrasonic experiments on suspensions of solid particles in liquids. The results of one of these series of experiments is shown in Figure 8. The host liquid was acetylene tetrabromide (ATB) and the solid particles in suspension were glass. Physical properties of the constituents are listed in Table 7. The solid curve in the Figure is the prediction of Wood's formula for these values. The agreement is again quite good.

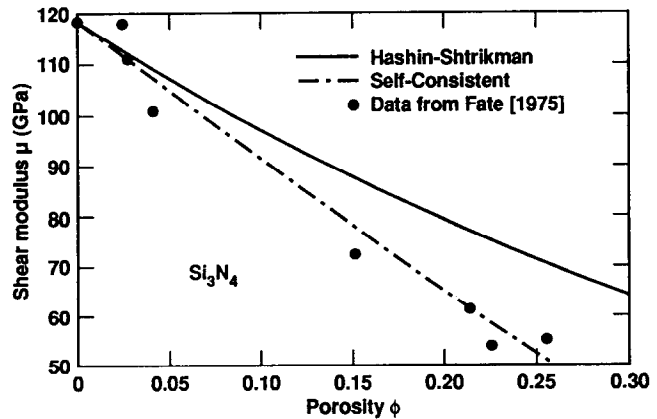


Fig. 5b. Shear modulus  $\mu$  of porous silicon nitride. Significance of the lines is the same as in FIG. 5A. Data from Fate [36].

TABLE 7. Material constants for constituents of some fluid mixtures and suspensions. Data from Kuster and Toksöz [56], Rossini *et al.* [83], and Wang and Nur [105].

Constituent	Velocity $V$ (km/sec)	Density $\rho$ (g/cc)	Bulk Modulus $K$ (GPa)
Water	1.500	1.000	2.25
Air	0.316	0.0012	$1.2 \times 10^{-4}$
1-Decene ( $C_{10}H_{20}$ )	1.247	0.7408	1.152
1-Octadecene ( $C_{18}H_{36}$ )	1.369	0.7888	1.478
ATB	1.025	2.365	2.485
Glass	6.790	2.405	76.71

## 5. THERMOELASTIC CONSTANTS

The equations of linear and isotropic thermoelasticity [13] are

$$\rho \frac{\partial^2 \mathbf{u}}{\partial t^2} = (\lambda + \mu) \nabla \nabla \cdot \mathbf{u} + \mu \nabla^2 \mathbf{u} - 3\alpha(\lambda + \frac{2}{3}\mu) \nabla \theta \quad (54)$$

and

$$\frac{1}{D} \frac{\partial \theta}{\partial t} + \beta \frac{\partial \nabla \cdot \mathbf{u}}{\partial t} = \nabla^2 \theta, \quad (55)$$

where  $\mathbf{u}$  is the vector of displacement,  $\theta$  is the increment of temperature,  $\lambda$  and  $\mu$  are the Lamé parameters,  $\alpha$  is the (linear) thermal expansion coefficient,  $D = k/C_v$  is the thermal diffusivity, and  $\beta = 3\alpha K \theta_0 / k$ , with  $C_v$  heat capacity at constant volume,  $\theta_0$  absolute temperature, and  $k$  thermal conductivity. The Lamé constants  $\lambda$  and  $\mu$  have the same significance as in linear elasticity and the bulk modulus is again  $K = \lambda + \frac{2}{3}\mu$ .

Detailed derivations of most of the results quoted here may be found in the textbook of Christensen [29]. The review articles by Hale [41] and Hashin [42] also discuss thermal expansion. Applications of thermoelasticity to rocks are discussed by McTigue [64] and Palciauskas and Domenico [73]. Ledbetter and Austin [61] have given an example of applications of the theory to data on a *SiC*-reinforced aluminum composite.

### 5.1. Exact

Levin's formula [62, 87] for the effective thermal expansion coefficient  $\alpha_{eff}$  for a two-component composite is given by

$$\frac{\alpha_{eff} - \alpha_2}{\alpha_1 - \alpha_2} = \frac{1/K_{eff} - 1/K_2}{1/K_1 - 1/K_2}, \quad (56)$$

where  $K_{eff}$  is the effective bulk modulus of the composite and  $\alpha_1, \alpha_2$  and  $K_1, K_2$  are, respectively, the thermal expansion coefficients and bulk moduli of the constituents. Equation (56) also implies that

$$\frac{\alpha_{eff} - \langle \alpha(\mathbf{r}) \rangle}{\alpha_1 - \alpha_2} = \frac{1/K_{eff} - \langle 1/K(\mathbf{r}) \rangle}{1/K_1 - 1/K_2}. \quad (57)$$

The corresponding exact results for specific heats [82] are

$$(C_p)_{eff} = \langle C_p(\mathbf{r}) \rangle + 9\theta_0 \left( \frac{\alpha_1 - \alpha_2}{1/K_1 - 1/K_2} \right)^2 \times \left( \frac{1}{K_{eff}} - \left\langle \frac{1}{K(\mathbf{r})} \right\rangle \right) \quad (58)$$

and

$$(C_v)_{eff} = (C_p)_{eff} - 9K_{eff}\alpha_{eff}^2\theta_0, \quad (59)$$

where  $C_p$  and  $C_v$  are the specific heats at constant pressure and constant volume, respectively, while  $\theta_0$  is the absolute temperature. In contrast, Kopp's law states that the specific heat of a solid element is the same whether it is free or part of a solid compound. Thus, Kopp's law implies that  $(C_p)_{eff} = \langle C_p(\mathbf{r}) \rangle$ , whereas the exact result for two components shows in-

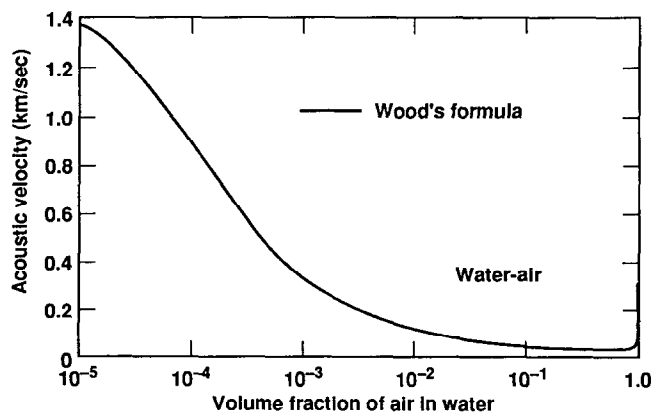


Fig. 6. Predicted acoustic velocities of water/air mixtures using Wood's formula (48).

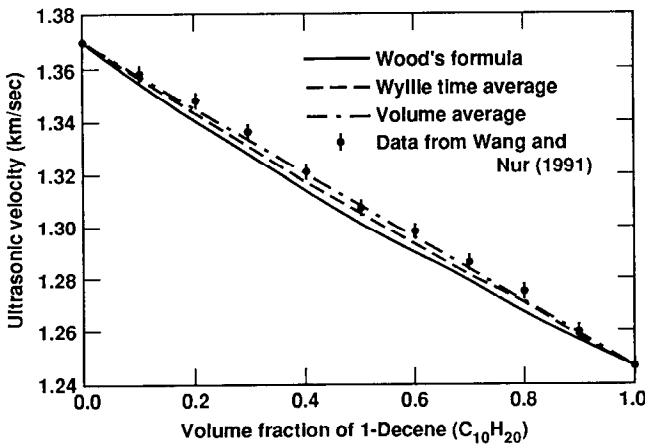


Fig. 7. Ultrasonic velocities of liquid hydrocarbon mixtures of 1-decene in 1-octadecene at room temperature. Data from Wang and Nur [105].

stead that there is a temperature dependent (but small for low temperatures) correction to this empirical law. Note that this correction (proportional to  $\theta_0$ ) is always negative, since the harmonic mean  $\langle 1/K \rangle^{-1}$  is a lower bound on  $K_{eff}$ .

## 5.2. Bounds

Levin [62] also used the Hashin-Shtrikman bounds on bulk modulus together with (56) to obtain bounds on  $\alpha_{eff}$ . When  $\alpha_1 > \alpha_2$ ,  $K_1 > K_2$ , and  $\mu_1 > \mu_2$ , the resulting bounds are

$$\frac{x_1 K_1 (3K_2 + 4\mu_2)}{3K_1 K_2 + 4\mu_2(x_1 K_1 + x_2 K_2)} \leq \frac{\alpha_{eff} - \alpha_2}{\alpha_1 - \alpha_2} \leq \frac{x_1 K_1 (3K_2 + 4\mu_1)}{3K_1 K_2 + 4\mu_1(x_1 K_1 + x_2 K_2)}, \quad (60)$$

or equivalently, using the function  $\Lambda$  defined in (3) with  $N = 2$ ,

$$\frac{1/\Lambda(\mu_2) - 1/\Lambda(0)}{1/K_1 - 1/K_2} \leq \frac{\alpha_{eff} - \langle \alpha(r) \rangle}{\alpha_1 - \alpha_2} \leq \frac{1/\Lambda(\mu_1) - 1/\Lambda(0)}{1/K_1 - 1/K_2}. \quad (61)$$

Rosen and Hashin [82] and Schapery [85] have obtained other (more complex) bounds on the effective thermal expansion coefficient.

Bounds on specific heat are shown by Christensen

[29] and Rosen and Hashin [82] to be

$$9\theta_0 \frac{\langle K(r)\alpha(r) \rangle^2}{\langle K(r) \rangle} \leq (C_p)_{eff} - \langle C_v(r) \rangle \leq 9\theta_0 \langle K(r)\alpha(r)^2 \rangle. \quad (62)$$

## 5.3. Estimates

Two simple estimates of the thermal expansion coefficient may be derived from (57) by applying the Reuss and Voigt bounds to  $K_{eff}$ . When  $K_{eff}$  is replaced by  $\langle 1/K(r) \rangle$  in (57), we obtain

$$\alpha^* = \langle \alpha(r) \rangle. \quad (63)$$

When  $K_{eff}$  is replaced by  $\langle K(r) \rangle$  in (57), we obtain

$$\alpha^* = \frac{\langle K(r)\alpha(r) \rangle}{\langle K(r) \rangle}. \quad (64)$$

In the two component case, these estimates are actually rigorous bounds – although which is the upper bound and which the lower one depends on the sign of the ratio  $(\alpha_1 - \alpha_2)/(K_1 - K_2)$ . When  $N > 2$ , we can use these formulas as general nonrigorous estimates. The second estimate (64) was first introduced by Turner [97].

Budiansky [24] and Laws [60] show that the self-consistent effective medium theory predicts the thermal expansion coefficient estimate is

$$\frac{K_{SC}^* \alpha_{SC}^*}{K_{SC}^* + \frac{4}{3}\mu_{SC}^*} = \left\langle \frac{K(r)\alpha(r)}{K(r) + \frac{4}{3}\mu_{SC}^*} \right\rangle \quad (65)$$

and the heat capacity estimate is

$$(C_v)_{SC}^* = \langle C_v(r) \rangle + \theta_0 \left\langle \frac{[K(r)\alpha(r) - K_{SC}^*\alpha_{SC}^*]^2}{K(r) + \frac{4}{3}\mu_{SC}^*} \right\rangle, \quad (66)$$

where  $K_{SC}^*$  and  $\mu_{SC}^*$  are given by (38). The correction term proportional to  $\theta_0$  is clearly always positive. Budiansky [24] and Duvall and Taylor [34] also give estimates of the effective Gruneisen constant ( $\gamma = K\alpha/C_v$ ) for a composite.

## 6. POREOELASTIC CONSTANTS (BIOT-GASSMANN THEORY)

Elastic response of solid/fluid mixtures is described by the equations of linear poroelasticity (also known

as Biot's equations [14–16]):

$$\rho \frac{\partial^2 \mathbf{u}}{\partial t^2} + \rho_f \frac{\partial^2 \mathbf{w}}{\partial t^2} = (H - \mu) \nabla \nabla \cdot \mathbf{u} + \mu \nabla^2 \mathbf{u} - C \nabla \zeta \quad (67)$$

and

$$\left( \frac{\rho_f \eta}{\kappa} \right) \frac{\partial \mathbf{w}}{\partial t} + \rho_f \frac{\partial^2 \mathbf{u}}{\partial t^2} = -\nabla p_f, \quad (68)$$

where  $\mathbf{u}$  is the solid displacement,  $\mathbf{w} = \phi(\mathbf{u} - \mathbf{u}_f)$  is the average relative fluid-solid displacement, the solid dilatation is  $e = \nabla \cdot \mathbf{u}$ , the increment of fluid content is  $\zeta = -\nabla \cdot \mathbf{w}$ , the fluid pressure is given by

$$p_f = M\zeta - Ce, \quad (69)$$

and the average density is

$$\rho = \phi \rho_f + (1 - \phi) \rho_{grain}. \quad (70)$$

When the porous solid is microhomogeneous (composed of only one type of solid grain), Gassmann [40] has shown that the principal elastic constant is given by

$$H = K_{undrained} + \frac{4}{3}\mu, \quad (71)$$

with the precise meaning of the remaining constants  $K_{undrained}$ ,  $M$  and  $C$  to be given below. The shear modulus of the porous solid frame is  $\mu$ . The density of the granular material composing the frame is  $\rho_{grain}$ . The bulk modulus and density of the saturating fluid are  $K_f$  and  $\rho_f$ . Kinematic viscosity of the fluid is  $\eta$ ; permeability of the porous frame is  $\kappa$ . We have used a low frequency simplification to obtain (68), since our main interest here is in quasistatic effects. Burridge and Keller [27] have shown that this macroscopic form of the equations follows from the coupling of the equations of linear elasticity and the Navier-Stokes equations at the microscopic level for a mixture of fluids and solids.

Results for poroelastic constants of porous composites (*i.e.*, for solid frames composed of multiple types of solid constituents) can be obtained by exploiting a rigorous analogy between poroelasticity and thermoelasticity [12, 70]; however, spatial constraints do not permit a discussion of this analogy here. Instead, we will first examine the mixture properties of the coefficients in the microhomogeneous case (containing only one mineral), since even in this rather simple problem we still have a mixture of fluid and solid; then we

TABLE 8. Ultrasonic velocities measured by Wang and Nur [105] for a sequence of binary hydrocarbon mixtures at 20° C compared to velocities computed using Wood's formula and Wyllie's time average equation. Table 7 contains the data required for computing Wood's formula. The formula for the 1-decene/1-octadecene hydrocarbon mixture is  $(C_{10}H_{20})_x(C_{18}H_{36})_{(1-x)}$ , where  $x$  is the volume fraction of 1-decene. Units of all velocities are km/s.

$x$	$V_{meas}$	$V_{Wood}$	$V_{Wyllie}$
0.00	1.369	1.369	1.369
0.10	1.358	1.354	1.356
0.20	1.348	1.340	1.343
0.294	1.336	1.328	1.331
0.40	1.321	1.314	1.317
0.50	1.307	1.301	1.305
0.60	1.298	1.290	1.293
0.70	1.286	1.279	1.281
0.80	1.275	1.267	1.270
0.90	1.260	1.257	1.258
1.00	1.247	1.247	1.247

consider the general properties of the coefficients for inhomogeneous rocks (containing two or more minerals).

The book on this subject by Bourbié *et al.* [17] is recommended.

## 6.1. Exact

**6.1.1. Microhomogeneous frame (one mineral).** Gassmann's formula for a microhomogeneous porous medium saturated with fluid wherein the fluid is confined to the pores during the deformation is

$$K_{undrained} = K_{drained} + (1 - K_{drained}/K_{grain})^2 M, \quad (72)$$

$$\frac{1}{M} = \frac{\phi}{K_f} + \frac{1 - \phi - K_{drained}/K_{grain}}{K_{grain}}, \quad (73)$$

and

$$C = (1 - K_{drained}/K_{grain})M. \quad (74)$$

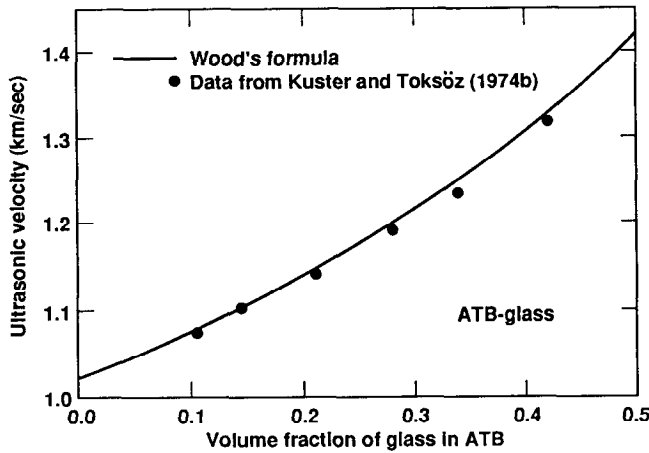


Fig. 8. Ultrasonic velocities in acetylene tetrabromide (ATB) with suspended particles of glass. Data from Kuster and Toksöz [56].

$K_{grain}$  is the bulk modulus of the granular material of which the porous frame is constituted, while  $K_{drained}$  is the bulk modulus of the porous solid frame defined by

$$\frac{1}{K_{drained}} = -\frac{1}{V} \left( \frac{\partial V}{\partial p_d} \right)_{p_f}. \quad (75)$$

$V$  is the total volume of the sample. The differential pressure  $p_d = p_c - p_f$  is the difference between the external (confining) pressure  $p_c$  and the fluid pressure  $p_f$ . The constant  $K_{drained}$  is sometimes known (see Stoll [90]) as the “jacketed bulk modulus.” The constant  $K_{undrained}$  is also sometimes known as the “confined” modulus or as the “saturated” modulus.

**6.1.2. Inhomogeneous frame (two or more minerals).** When the porous solid composing the frame is not microhomogeneous, Gassmann’s equation is no longer strictly applicable, although it is commonly applied by introducing an averaged bulk modulus for  $K_{grain}$  in the formulas. This procedure is not quite correct however. Rigorous generalizations of Gassmann’s equation have been discussed by Brown and Korringa [20] and Rice and Cleary [81].

The result for  $K_{undrained}$  is again of the form

$$K_{undrained} = K_{drained} + (1 - K_{drained}/K_s)^2 M, \quad (76)$$

where now

$$\frac{1}{M} = \phi \left( \frac{1}{K_f} - \frac{1}{K_\phi} \right) + \frac{(1 - K_{drained}/K_s)}{K_s} \quad (77)$$

and

$$C = (1 - K_{drained}/K_s) M. \quad (78)$$

The frame constant  $K_{drained}$  is defined as before in (75) and  $K_s$  and  $K_\phi$  are defined by

$$\frac{1}{K_s} = -\frac{1}{V} \left( \frac{\partial V}{\partial p_f} \right)_{p_d}, \quad (79)$$

and

$$\frac{1}{K_\phi} = -\frac{1}{V_\phi} \left( \frac{\partial V_\phi}{\partial p_f} \right)_{p_d}, \quad (80)$$

where  $V_\phi = \phi V$  is the pore volume. The modulus  $K_s$  is sometimes called (see Stoll [90]) the “unjacketed bulk modulus.” The modulus  $K_\phi$  is the effective bulk modulus of the pore volume.

## 6.2. Bounds

**6.2.1. Microhomogeneous frame.** Since the Voigt and Reuss bounds show that  $0 \leq K_{drained} \leq (1 - \phi)K_{grain}$  and since the right hand side of (72) is a monotonically increasing function of  $K_{drained}$ , it is straightforward to show that

$$\begin{aligned} \left( \frac{\phi}{K_f} + \frac{1 - \phi}{K_{grain}} \right)^{-1} &\leq K_{undrained} \\ &\leq \phi K_f + (1 - \phi) K_{grain}. \end{aligned} \quad (81)$$

Thus,  $K_{undrained}$  is bounded above and below by appropriate Voigt and Reuss bounds.

As a function of  $K_{grain}$ ,  $K_{undrained}$  is also a monotonically increasing function of  $K_{grain}$ . Using the fact that  $K_{drained}/(1 - \phi) \leq K_{grain} \leq \infty$ , we find

$$\phi K_f \leq K_{undrained} - K_{drained} \leq K_f/\phi. \quad (82)$$

**6.2.2. Inhomogeneous frame.** Since  $K_{undrained}$  is a monotonically increasing function of  $K_{drained}$ , we obtain bounds on  $K_{undrained}$  by considering the inequalities  $0 \leq K_{drained} \leq (1 - \phi)K_s$ , where the lower bound is rigorous and the upper bound is empirical. We find that

$$\begin{aligned} \left[ \frac{1}{K_s} + \phi \left( \frac{1}{K_f} - \frac{1}{K_\phi} \right) \right]^{-1} &\leq K_{undrained} \\ &\leq (1 - \phi)K_s + \phi \left[ \frac{1}{K_f} + \left( \frac{1}{K_s} - \frac{1}{K_\phi} \right) \right]^{-1} \end{aligned} \quad (83)$$

which reduces to (81) if  $K_s = K_\phi = K_{grain}$ .

TABLE 9. Material constants for constituents of some solid/fluid mixtures. Data from Plona [77] and Murphy [69].

Constituent	Velocity $V_+$ (km/sec)	Velocity $V_s$ (km/sec)	Density $\rho$ (g/cc)	Bulk Modulus $K$ (GPa)	Shear Modulus $\mu$ (GPa)
Water	1.49	—	0.997	2.2	—
Air	0.32	—	0.0012	$1.2 \times 10^{-4}$	—
Glass	5.69	3.46	2.48	40.7	29.7
Sand grains	5.08	3.07	2.65	35.0	25.0

Since  $K_{undrained}$  is also a monotonically increasing function of  $K_s$  if  $M \leq K_s$  (which is generally true), we can obtain bounds on  $K_{undrained}$  by considering  $K_{drained}/(1 - \phi) \leq K_s \leq \infty$ , where the lower bound is empirical and the upper bound is rigorous. We find that

$$\begin{aligned} \phi^2 \left[ \phi \left( \frac{1}{K_f} - \frac{1}{K_\phi} \right) + \frac{(1 - \phi)}{K_{drained}} \right]^{-1} \\ \leq K_{undrained} - K_{drained} \\ \leq \left[ \phi \left( \frac{1}{K_f} - \frac{1}{K_\phi} \right) \right]^{-1}. \quad (84) \end{aligned}$$

If  $K_\phi$  is positive, thermodynamic stability [12] requires that  $\phi K_s / (1 - K_{drained}/K_s) \leq K_\phi \leq \infty$ . The generalized Gassmann formula for  $K_{undrained}$  is also a monotonically decreasing function of  $K_\phi$ , so we find

$$\begin{aligned} \left( \frac{\phi}{K_f} + \frac{(1 - K_{drained}/K_s)}{K_s} \right)^{-1} \\ \leq \frac{K_{undrained} - K_{drained}}{(1 - K_{drained}/K_s)^2} \leq K_f/\phi. \quad (85) \end{aligned}$$

### 6.3. Estimates

Various approximations for the coefficients in the equations of poroelasticity have been discussed by Buidansky and O'Connell [25, 26], Thomsen [94], and Berryman [9].

### 6.4. Examples

We consider two examples of applications of Biot's theory to real porous materials. Since both cases involve ultrasonic experiments, equation (68) must be generalized to take account of some higher frequency effects. To do this, we introduce the Fourier transform (assuming time dependence of the form  $\exp -i\omega t$ ) of

both (67) and (68), and then replace the coefficient of the first term in (68) so we have

$$-\omega^2 [q(\omega)\mathbf{w} + \rho_f \mathbf{u}] = -\nabla p_f, \quad (86)$$

where the coefficient

$$q(\omega) = \frac{\tau \rho_f}{\phi} + iQ(\xi) \frac{\rho_f \eta}{\kappa \omega}. \quad (87)$$

The electric tortuosity is  $\tau$ . The definition of the complex function  $Q(\xi)$  may be found in Biot [15]. The argument  $\xi = (\omega h^2/\eta)^{1/2}$  depends on a length parameter  $h$  playing the role of hydraulic radius.

Some of the constituent data required for these examples is displayed in Table 9.

**6.4.1. Fluid-saturated porous glass.** Plona [77] observed two distinct compressional waves in a water-saturated, porous structure made from sintered glass beads (see Table 10). The speeds predicted by Biot's equations of poroelasticity are compared to the values observed by Plona shown in Figure 9.

The input parameters to the model are  $K_s = 40.7$  GPa,  $\mu_s = 29.7$  GPa,  $\rho_s = 2.48$  g/cc,  $K_f = 2.2$  GPa,  $\rho_f = 1.00$  g/cc,  $\nu = 1.00$  centistoke, and  $\omega = 2\pi \times 500$  kHz. The frame moduli  $K$  and  $\mu$  were calculated assuming spherically shaped glass particles and needle-shaped inclusions of voids. We use  $\tau = \phi^{-1/2}$  for the tortuosity. The permeability variation with porosity was taken to obey the Kozeny-Carman relation

$$\kappa = \text{const} \times \phi^3 / (1 - \phi)^2, \quad (88)$$

which has been shown empirically to provide a reasonable estimate of the porosity variation of permeability. We choose  $\kappa_0 = 9.1 \times 10^{-8}$  cm<sup>2</sup> ( $\simeq 9.1$  D) at  $\phi_0 = 0.283$  and then use (88) to compute the value of  $\kappa$  for all other porosities considered. No entirely satisfactory model for the characteristic length  $h$  has been

TABLE 10. Values of poroelastic wave speeds in porous glass at 2.25 MHz. All velocities have dimensions of km/sec. Data from Plona [77], Johnson and Plona [53], and Plona and Johnson [78].

Porosity $\phi$	Experiment	Theory	Experiment	Theory	Experiment	Theory
	$V_+$	$V_+$	$V_s$	$V_s$	$V_-$	$V_-$
0.000	5.69	5.69	3.46	3.46	—	0.00
0.075	5.50	5.33	3.31	3.22	—	0.52
0.105	5.15	5.17	2.97	3.12	0.58	0.65
0.162	4.83	4.86	2.68	2.92	0.70	0.77
0.185	4.84	4.72	2.93	2.83	0.82	0.79
0.219	4.60	4.50	2.68	2.68	0.88	0.82
0.258	4.18	4.22	2.50	2.50	1.00	0.85
0.266	3.98	4.15	2.21	2.46	0.94	0.86
0.283	4.05	4.02	2.37	2.36	1.04	0.87
0.335	3.19	3.53	1.68	2.04	0.99	0.90
0.380	2.81	3.01	1.41	1.67	0.96	0.90

found. However, dimensional analysis suggests that  $h^2$  must be comparable to  $\kappa$ , so we have taken

$$h^2/\kappa = h_0^2/\kappa_0 = \text{const.} \quad (89)$$

At  $\phi_0 = 0.283$ , we choose  $h_0 = 0.02$  mm corresponding

to an average pore radius  $\frac{1}{5}$  to  $\frac{1}{7}$  of the grain radius (the glass beads in Plona's samples were 0.21–0.29 mm in diameter before sintering).

The theoretical results for the fast compressional wave and the shear wave agree with Plona's measurements within the experimental error ( $\pm 3\%$  relative error in measured speeds and an absolute error of  $\pm 0.005$  in measured porosity).

**6.4.2. Massilon sandstone.** Murphy [69] has presented data on compressional and shear velocities in partially saturated Massilon sandstone. To calculate the expected behavior of the compressional and shear velocities as a function of water content, the pore fluid is taken to be a water/air mixture with bulk modulus given by the harmonic mean and density given by the volume average as in Wood's formula. The parameters used in the calculations are  $K = 1.02$  GPa,  $\mu = 1.44$  GPa,  $K_s = 35.0$  GPa,  $\mu_s = 25.0$  GPa,  $\rho_s = 2.65$  g/cc,  $K_l = 2.25$  GPa,  $\rho_l = 0.997$  g/cc,  $K_g = 1.45 \times 10^{-4}$  GPa,  $\rho = 1.20 \times 10^{-3}$  g/cc,  $\phi = 0.23$ ,  $\kappa = 260$  mD,  $h = 15\mu\text{m}$ , and  $\omega = 2\pi \times 560$  Hz. The electrical tortuosity has value  $\tau = 2.76$ . The values of  $K$  and  $\mu$  for the frame were chosen to fit the experimental data at full water saturation. The remaining points of the theoretical curve (the solid lines) in Figure 10 follow without further adjustment of parameters. The agreement between theory and experiment is quite good for this example. The observed agreement is as much a confirmation of Wood's formula as it is of the equations of poroelasticity.

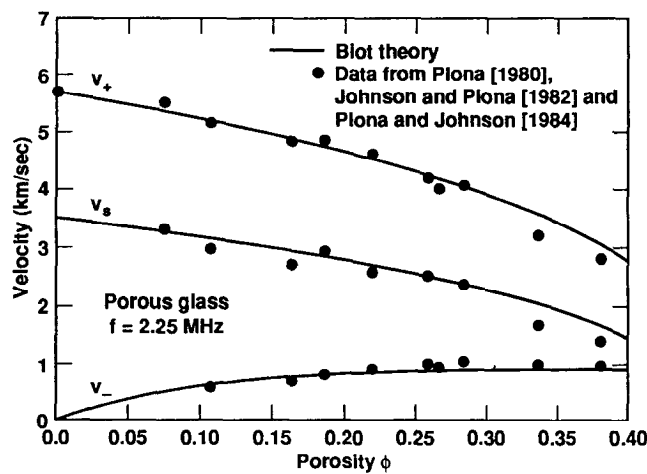


Fig. 9. Ultrasonic velocities (slow compressional –  $v_-$ , shear –  $v_s$ , fast compressional –  $v_+$ ) in water-saturated porous glass. Theoretical curves from Biot's theory as described in the text. Data from Plona [77], Johnson and Plona [53], and Plona and Johnson [78].

## 7. FLUID PERMEABILITY (DARCY'S CONSTANT)

A qualitative difference between fluid permeability (also known as hydraulic conductivity or Darcy's constant) and other transport properties such as electrical or thermal conductivity is that the pertinent macroscopic equation (Darcy's law) does not have the same form as the microscopic equation (Navier-Stokes equation).

A porous medium of total volume  $V$  filled with a fluid occupying the pore volume  $V_\phi$  has an applied stress tensor  $\Pi_{ij}$  known on the exterior boundary. The applied stress takes the form

$$\Pi_{ij} = -p_f \delta_{ij} + \tau_{ij}, \quad (90)$$

where the viscosity tensor  $\tau_{ij}$  is related to the fluid velocity field  $v_i$  by

$$\tau_{ij} = \rho_f \eta (v_{i,j} + v_{j,i}) \quad \text{for } i, j = 1, 2, 3. \quad (91)$$

In this notation,  $i$  and  $j$  index the directions in a cartesian coordinate system ( $x = x_1$ ,  $y = x_2$ ,  $z = x_3$ ) and the subscript appearing after a comma refers to a partial derivative: thus,  $v_{2,3} = \partial v_2 / \partial z$ . The fluid pressure is  $p_f$  and the fluid viscosity is  $\rho_f \eta$ . The energy dissipation in the fluid is given by [57]

$$\mathcal{D} = \frac{1}{2\rho_f \eta V} \int_{V_\phi} \tau_{i,j} \tau_{i,j} d^3x \geq 0, \quad (92)$$

where the summation convention is assumed for repeated indices in (92).

Neglecting body forces (e.g., gravity) and supposing the macroscopic applied pressure gradient arises due to the pressure difference  $\Delta P$  across a distance  $\Delta Z$  in the direction  $\hat{z}$ , the relationship between the microscopic stresses and the macroscopic forces is given by

$$\mathcal{D} = \frac{\kappa}{\rho_f \eta} \left( \frac{\Delta P}{\Delta Z} \right)^2 \quad (93)$$

or equivalently

$$\mathcal{D} = -\mathbf{J} \cdot \hat{z} \frac{\Delta P}{\Delta Z}, \quad (94)$$

where  $\mathbf{J}$  is the volumetric flow rate per unit area and

$$\mathbf{J} = -\hat{z} \frac{\kappa}{\rho_f \eta} \frac{\Delta P}{\Delta Z} = -\frac{\kappa}{\rho_f \eta} \nabla p_f. \quad (95)$$

Equation (95) is Darcy's law in the absence of body forces. The new constant appearing in (93) and (95)

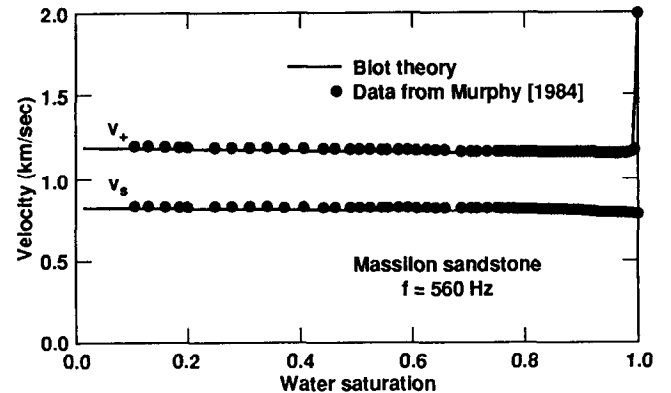


Fig. 10. Ultrasonic velocities (shear –  $v_s$ , fast compressional –  $v_+$ ) in partially saturated Massilon sandstone. Theoretical curves from Biot's theory as described in the text. Data from Murphy [69].

is the fluid permeability or Darcy's constant  $\kappa$ . Although the macroscopic equation (95) has the same form as that discussed in Section 2, the fact that the microscopic equation has a different form from that of the macroscopic equation makes it essential to perform a separate analysis for this problem. A key difference is the no-slip boundary condition for fluid flow through porous media.

General references on fluid flow through porous media are Bear [4], Dullien [33], and Adler [1].

### 7.1. Bounds

Most bounds on fluid permeability [10, 84] require knowledge of the geometrical arrangement of solid material and are therefore beyond the scope of the present review.

One exception to this rule is the variational bound of Weissberg and Prager [109] derived for a particularly simple model of a random composite called the "penetrable sphere model." The penetrable sphere model is a theoretical construct for which exact information is available about the statistics of the microgeometry [96]. The model is constructed by throwing points randomly in a box and then letting spheres grow around the points until the desired porosity is reached. The result of Weissberg and Prager [109] is

$$\kappa \leq -\frac{2}{9} \frac{\phi R^2}{\ln \phi}, \quad (96)$$

where  $R$  is the radius of the spheres and  $\phi$  is the porosity.

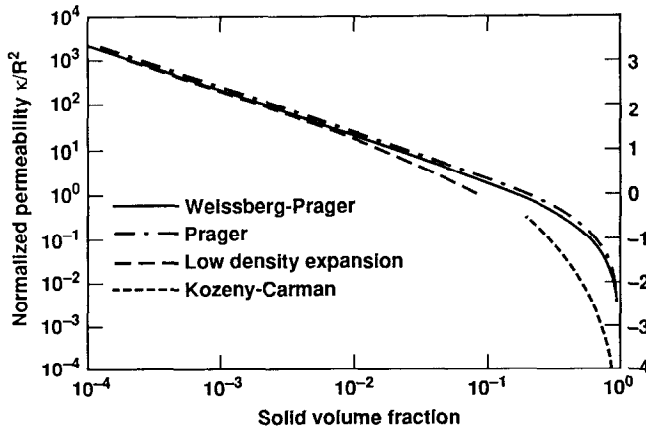


Fig. 11. Bounds and estimates on normalized permeability  $\kappa/R^2$  for the penetrable sphere model. Various equations used are defined in the text.

## 7.2. Estimates

**7.2.1. Kozeny-Carman model.** Empirical formulas for fluid permeability associated with the names of Kozeny and Carman are common [74,103]. One typical example of such a formula is

$$\kappa = \frac{\phi^2}{2s^2F}, \quad (97)$$

where  $\phi$  is the porosity,  $s$  is the specific surface area for an equivalent smooth-walled pore, and  $F$  is the electrical formation factor (ratio of the conductivity of a saturating pore fluid to the overall conductivity of the saturated sample).

**7.2.2. Series expansion method.** Among the well-known estimates of permeability are those due to Brinkman [19], Childress [28], Howells [50], and Hinch [49]. The low density expansion for the permeability

of a random assemblage of hard spheres has the form

$$\begin{aligned} \kappa_{Stokes}/\kappa &= 1 + \frac{3}{\sqrt{2}}(1-\phi)^{\frac{1}{2}} \\ &+ \frac{135}{64}(1-\phi)\ln(1-\phi) + 16.5(1-\phi) + \dots, \end{aligned} \quad (98)$$

where the exact result for Stokes flow through a dilute assemblage of spheres of radius  $R$  is

$$\kappa_{Stokes} = \frac{2R^2}{9(1-\phi)}. \quad (99)$$

## 7.3. Examples

**7.3.1. Penetrable sphere model.** Results for the penetrable sphere model [96] are shown in Figure 11. The solid volume fraction is  $1-\phi$  and  $\kappa/R^2$  is the normalized permeability, where  $R$  is the radius of the spheres in the model. The Kozeny-Carman empirical relation used in the plot is

$$\kappa_{Stokes}/\kappa_{KC} = 10(1-\phi)/\phi^3, \quad (100)$$

where the Stokes permeability in a dilute assemblage of spheres of radius  $R$  is given by (99). The formula of Weissberg and Prager [109] appears in (96), while the results for the Prager [79] bound have been taken from numerical results found in Berryman and Milton [10]. The series expansion results are given by (98).

*Acknowledgments.* I thank P. A. Berge, G. M. Mavko, G. W. Milton, and R. W. Zimmerman for helpful conversations. This work was performed under the auspices of the U. S. Department of Energy by the Lawrence Livermore National Laboratory under contract No. W-7405-ENG-48 and supported specifically by the Geosciences Research Program of the DOE Office of Energy Research within the Office of Basic Energy Sciences, Division of Engineering and Geosciences.

## REFERENCES

1. Adler, P. M., *Porous Media - Geometry and Transports*, 544 pp., Butterworth-Heinemann, Boston, MA, 1992.
2. Backus, G. E., Long-wave elastic anisotropy produced by horizontal layering, *J. Geophys. Res.*, **67**, 4427–4440, 1962.
3. Batchelor, G. K., Transport properties of two-phase materials with random structure, in *Annual Reviews of Fluid Mechanics*, Vol. 6, edited by M. Van Dyke, W. G. Vincenti, and J. V. Wehausen, pp. 227–255, Annual Reviews, Palo Alto, CA, 1974.
4. Bear, J., *Dynamics of Fluids in Porous Media*, 764 pp., Elsevier, New York, 1972.
5. Beran, M. J., *Statistical Continuum Theories*, 424 pp., Wiley, New York, 1968.
6. Bergman, D. J., The dielectric constant of a composite material - A problem in classical physics, *Physics Reports*, **43**, 377–407, 1978.
7. Berryman, J. G., Long-wavelength propagation in composite elastic media, *J. Acoust. Soc. Am.*, **68**, 1809–1831, 1980.
8. Berryman, J. G., Effective medium theory for elastic composites, in *Elasticity and wave propagation in layered media*, edited by J. G. Berryman and G. M. Mavko, pp. 1–20, Springer-Verlag, Berlin, 1991.

- tic Wave Scattering and Propagation*, edited by V. K. Varadan and V. V. Varadan, pp. 111–129, Ann Arbor Science, Ann Arbor, Michigan, 1982.
9. Berryman, J. G., Single-scattering approximations for coefficients in Biot's equations of poroelasticity, *J. Acoust. Soc. Am.*, **91**, 551–571, 1992.
  10. Berryman, J. G., and G. W. Milton, Normalization constraint for variational bounds on fluid permeability, *J. Chem. Phys.*, **83**, 754–760, 1985.
  11. Berryman, J. G., and G. W. Milton, Microgeometry of random composites and porous media, *J. Phys. D: Appl. Phys.*, **21**, 87–94, 1988.
  12. Berryman, J. G., and G. W. Milton, Exact results for generalized Gassmann's equations in composite porous media with two constituents, *Geophysics*, **56**, 1950–1960, 1991.
  13. Biot, M. A., Thermoelasticity and irreversible thermodynamics, *J. Appl. Phys.*, **27**, 240–253, 1956a.
  14. Biot, M. A., Theory of propagation of elastic waves in a fluid-saturated porous solid. I. Low-frequency range, *J. Acoust. Soc. Am.*, **28**, 168–178, 1956b.
  15. Biot, M. A., Theory of propagation of elastic waves in a fluid-saturated porous solid. II. Higher frequency range, *J. Acoust. Soc. Am.*, **28**, 179–191, 1956c.
  16. Biot, M. A., Mechanics of deformation and acoustic propagation in porous media, *J. Appl. Phys.*, **33**, 1482–1498, 1962.
  17. Bourbié, T., O. Coussy, and B. Zinszner, *Acoustics of Porous Media*, 334 pp., Chapter 3, Gulf, Houston, 1987.
  18. Brace, W. F., Some new measurements of linear compressibility of rocks, *J. Geophys. Res.*, **70**, 391–398, 1965.
  19. Brinkman, H. C., A calculation of the viscous force exerted by a flowing fluid on a dense swarm of particles, *Appl. Sci. Res.*, **A1**, 27–34, 1947.
  20. Brown, R. J. S., and J. Korringa, On dependence of the elastic properties of a porous rock on the compressibility of a pore fluid, *Geophysics*, **40**, 608–616, 1975.
  21. Brown, W. F., Jr., Dielectric constants, permeabilities, and conductivities of random media, *Trans. Soc. Rheol.*, **9**, 357–380, 1965.
  22. Bruggeman, D. A. G., Berechnung verschiedener physikalischer Konstanten von heterogenen Substanzen, *Ann. Physik. (Leipzig)*, **24**, 636–679, 1935.
  23. Budiansky, B., On the elastic moduli of some heterogeneous materials, *J. Mech. Phys. Solids*, **13**, 223–227, 1965.
  24. Budiansky, B., Thermal and thermoelastic properties of isotropic composites, *J. Comp. Mater.*, **4**, 286–295, 1970.
  25. Budiansky, B., and R. J. O'Connell, Elastic moduli of dry and saturated cracked solids, *Int. J. Solids Struct.*, **12**, 81–97, 1976.
  26. Budiansky, B., and R. J. O'Connell, Bulk dissipation in heterogeneous media, in *Solid Earth Geophysics and Geotechnology*, edited by S. Nemat-Nasser, pp. 1–10, ASME, New York, 1980.
  27. Burridge, R., and J. B. Keller, Poroelasticity equations derived from microstructure, *J. Acoust. Soc. Am.*, **70**, 1140–1146, 1981.
  28. Childress, S., Viscous flow past a random array of spheres, *J. Chem. Phys.*, **56**, 2527–2539, 1972.
  29. Christensen, R. M., *Mechanics of Composite Materials*, 348 pp., Chapter IX, pp. 311–339, Wiley, New York, 1979.
  30. Chung, D.-H., Elastic moduli of single crystal and polycrystalline  $MgO$ , *Phil. Mag.*, **8**, 833–841, 1963.
  31. Cleary, M. P., I.-W. Chen, and S.-M. Lee, Self-consistent techniques for heterogeneous media, *ASCE J. Eng. Mech.*, **106**, 861–887, 1980.
  32. Cohen, R. W., G. D. Cody, M. D. Coutts, and B. Abeles, Optical properties of granular silver and gold films, *Phys. Rev. B*, **8**, 3689–3701, 1973.
  33. Dullien, F. A. L., *Porous Media: Fluid Transport and Pore Structure*, 574 pp., Chapter 3, Academic Press, San Diego, 1992.
  34. Duvall, G. E., and S. M. Taylor, Jr., Shock parameters in a two component mixture, *J. Composite Mat.*, **5**, 130–139, 1971.
  35. Eshelby, J. D., The determination of the elastic field of an ellipsoidal inclusion, and related problems, *Proc. Roy. Soc. London A*, **241**, 376–396, 1957.
  36. Fate, W. A., High temperature elastic moduli of polycrystalline silicon nitride, *J. Appl. Phys.*, **46**, 2375–2377, 1975.
  37. Fisher, E. S., M. H. Manghnani, and J. L. Routbort, A study of the elastic properties of  $Al_2O_3$  and  $Si_3N_4$  matrix composites with  $SiC$  whisker reinforcement, in *High Performance Composites for the 1990's*, edited by S. K. Das, C. P. Ballard, and F. Maastrikar, pp. 365–370, The Minerals, Metals and Materials Society, Warrendale, Pennsylvania, 1991.
  38. Fisher, E. S., M. H. Manghnani, and J.-F. Wang, Elastic properties of  $Al_2O_3$  and  $Si_3N_4$  matrix composites with  $SiC$  whisker reinforcement, *J. Am. Ceramics Soc.*, **75**, 908–914, 1992.
  39. Galeener, F. L., Optical evidence for a network of cracklike voids in amorphous germanium, *Phys. Rev. Lett.*, **27**, 1716–1719, 1971.
  40. Gassmann, F., Über die Elastizität poröser medien, *Veiteler Jahrrsschrift der Naturforschenden Gesellschaft in Zürich*, **96**, 1–23, 1951.
  41. Hale, D. K., The physical properties of composite materials, *J. Mater. Sci.*, **11**, 2105–2141, 1976.
  42. Hashin, Z., Analysis of composite materials – a survey, *ASME J. Appl. Mech.*, **50**, 481–505, 1983.
  43. Hashin, Z., and S. Shtrikman, Note on a variational approach to the theory of composite elastic materials, *J. Franklin Inst.*, **271**, 336–341, 1961.
  44. Hashin, Z., and S. Shtrikman, A variational approach to the theory of the effective magnetic permeability of

- multiphase materials, *J. Appl. Phys.*, **33**, 3125–3131, 1962a.
45. Hashin, Z., and S. Shtrikman, A variational approach to the theory of elastic behaviour of polycrystals, *J. Mech. Phys. Solids*, **10**, 343–352, 1962b.
46. Hill, R., The elastic behaviour of crystalline aggregate, *Proc. Phys. Soc. London*, **A65**, 349–354, 1952.
47. Hill, R., Elastic properties of reinforced solids: Some theoretical principles, *J. Mech. Phys. Solids*, **11**, 357–372, 1963.
48. Hill, R., A self-consistent mechanics of composite materials, *J. Mech. Phys. Solids*, **13**, 213–222, 1965.
49. Hinch, E. J., An averaged-equation approach to particle interactions, *J. Fluid Mech.*, **83**, 695–720, 1977.
50. Howells, I. D., Drag due to the motion of a Newtonian fluid through a sparse random array of small fixed rigid objects, *J. Fluid Mech.*, **64**, 449–475, 1974.
51. Hudson, J. A., Overall properties of heterogeneous material, *Geophys. J. Int.*, **107**, 505–511, 1991.
52. Jackson, J. D., *Classical Electrodynamics*, pp. 118–119, Wiley, New York, 1962.
53. Johnson, D. L., and T. J. Plona, Acoustic slow waves and the consolidation transition, *J. Acoust. Soc. Am.*, **72**, 556–565, 1982.
54. Johnson, D. L., T. J. Plona, C. Scala, F. Pasierb, and H. Kojima, Tortuosity and acoustic slow waves, *Phys. Rev. Lett.*, **49**, 1840–1844, 1982.
55. Kuster, G. T., and M. N. Toksöz, Velocity and attenuation of seismic waves in two-phase media: Part I. Theoretical formulations, *Geophysics*, **39**, 587–606, 1974a.
56. Kuster, G. T., and M. N. Toksöz, Velocity and attenuation of seismic waves in two-phase media: Part II. Experimental results, *Geophysics*, **39**, 607–618, 1974b.
57. Landau, L. D., and E. M. Lifshitz, *Fluid Mechanics*, pp. 53–54, Pergamon, London, 1959.
58. Landauer, R., The electrical resistance of binary metallic mixtures, *J. Appl. Phys.*, **23**, 779–784, 1952.
59. Landauer, R., Electrical conductivity in inhomogeneous media, in *Electrical, Transport, and Optical Properties of Inhomogeneous Media*, edited by J. C. Garland and D. B. Tanner, pp. 2–43, Proceedings of the Conference at Ohio State University, September, 1977, American Institute of Physics, New York, 1978.
60. Laws, N., On the thermostatics of composite materials, *J. Mech. Phys. Solids*, **21**, 9–17, 1973.
61. Ledbetter, H., and M. Austin, Thermal expansion of an SiC particle-reinforced aluminum composite, *Int. J. Thermophys.*, **12**, 731–739, 1991.
62. Levin, V. M., Thermal expansion coefficients of heterogeneous materials, *Mech. Solids*, **2**, 58–61, 1967.
63. Mackensie, J. K., The elastic constants of a solid containing spherical holes, *Proc. Phys. Soc. London B*, **63**, 2–11, 1950.
64. McTigue, D. F., Thermoelastic response of fluid-saturated porous rock, *J. Geophys. Res.*, **91**, 9533–9542, 1986.
65. Milton, G. W., The coherent potential approximation is a realizable effective medium scheme, *Comm. Math. Phys.*, **99**, 463–500, 1985.
66. Milton, G. W., and R. V. Kohn, Variational bounds on the effective moduli of anisotropic composites, *J. Mech. Phys. Solids*, **36**, 597–629, 1988.
67. Molyneux, J. E., Effective permittivity of a polycrystalline dielectric, *J. Math. Phys.*, **11**, 1172–1184, 1970.
68. Molyneux, J. E., and M. J. Beran, Statistical properties of the stress and strain fields in a medium with small random variations in elastic coefficients, *J. Math. Mech.*, **14**, 337–351, 1965.
69. Murphy, W. F., III, Acoustic measures of partial gas saturation in tight sandstones, *J. Geophys. Res.*, **89**, 11549–11559, 1984.
70. Norris, A. N., On the correspondence between poroelasticity and thermoelasticity, *J. Appl. Phys.*, **71**, 1138–1141, 1992.
71. Norris, A. N., P. Sheng, and A. J. Callegari, Effective-medium theories for two-phase dielectric media, *J. Appl. Phys.*, **57**, 1990–1996, 1985.
72. Osborn, J. A., Demagnetizing factors of the general ellipsoid, *Phys. Rev.*, **67**, 351–357, 1945.
73. Palciauskas, V. V., and P. A. Domenico, Characterization of drained and undrained response of thermally loaded repository rocks, *Water Resources Res.*, **18**, 281–290, 1982.
74. Paterson, M. S., The equivalent channel model for permeability and resistivity in fluid-saturated rocks – A reappraisal, *Mech. Mater.*, **2**, 345–352, 1983.
75. Peselnick, L., Elastic constants of Solenhofen limestone and their dependence upon density and saturation, *J. Geophys. Res.*, **67**, 4441–4448, 1962.
76. Peselnick, L., and R. Meister, Variational method of determining effective moduli of polycrystals: (A) Hexagonal symmetry and (B) trigonal symmetry, *J. Appl. Phys.*, **36**, 2879–2884, 1965.
77. Plona, T. J., Observation of a second bulk compressional wave in a porous medium at ultrasonic frequencies, *Appl. Phys. Lett.*, **36**, 259–261, 1980.
78. Plona, T. J., and D. L. Johnson, Acoustic properties of porous systems: I. Phenomenological description, in *Physics and Chemistry of Porous Media*, edited by D. L. Johnson and P. N. Sen, pp. 89–104, American Institute of Physics, New York, 1984.
79. Prager, S., Viscous flow through porous media, *Phys. Fluids*, **4**, 1477–1482, 1961.
80. Reuss, A., Berechnung der Fließgrenze von Mischkristallen, *Z. Angew. Math. Mech.*, **9**, 55, 1929.
81. Rice, J. R., and M. P. Cleary, Some basic stress diffusion solutions for fluid-saturated elastic porous media with compressible constituents, *Rev. Geo-*

- phys. Space Phys.*, **14**, 227-241, 1976.
82. Rosen, B. W., and Z. Hashin, Effective thermal expansion coefficients and specific heats of composite materials, *Int. J. Engng. Sci.*, **8**, 157-173, 1970.
83. Rossini, F. D., K. S. Pitzer, R. L. Arnet, R. M. Braun, and G. C. Pimentel, *Selected Values of Physical and Thermodynamic Properties of Hydrocarbons and Related Compounds*, p. 52, Carnegie Press, Pittsburgh, Pennsylvania, 1953.
84. Rubinstein, J., and S. Torquato, Flow in random porous media: mathematical formulation, variational principles, and rigorous bounds, *J. Fluid Mech.*, **206**, 25-46, 1989.
85. Schapery, R. A., Thermal expansion coefficients of composite materials based on energy principles, *J. Comp. Mater.*, **2**, 380-404, 1968.
86. Schulgasser, K., Bounds on the conductivity of statistically isotropic polycrystals, *J. Phys. C*, **10**, 407-417, 1977.
87. Schulgasser, K., Thermal expansion of polycrystals, *J. Material Sci. Lett.*, **8**, 228-229, 1989.
88. Sen, P. N., C. Scala, and M. H. Cohen, A self-similar model for sedimentary rocks with application to the dielectric constant of fused glass beads, *Geophysics*, **46**, 781-795, 1981.
89. Simmons, G., and H. Wang, *Single Crystal Elastic Constants and Calculated Aggregate Properties: A Handbook*, 300 pp. MIT Press, Cambridge, MA, 1971.
90. Stoll, R. D., Acoustic waves in saturated sediments, in *Physics of Sound in Marine Sediments*, edited by L. Hampton, pp. 19-39, Plenum, New York, 1974.
91. Stoner, E. C., The demagnetizing factors for ellipsoids, *Phil. Mag.*, **36**, 803-821, 1945.
92. Stroud, D., Generalized effective-medium approach to the conductiv-  
*Phys. Rev. B*, **12**, 3368-3373, 1975.
93. Thomsen, L., Elasticity of polycrystals and rocks, *J. Geophys. Res.*, **77**, 315-327, 1972.
94. Thomsen, L., Biot-consistent elastic moduli of porous rocks: Low-frequency limit, *Geophysics*, **50**, 2797-2807, 1985.
95. Torquato, S., Random heterogeneous media: Microstructure and improved bounds on effective properties, *Appl. Mech. Rev.*, **44**, 37-76, 1991.
96. Torquato, S., and G. Stell, Microstructure of two-phase random media. III. The  $n$ -point matrix probability functions for fully penetrable spheres, *J. Chem. Phys.*, **79**, 1505-1510, 1983.
97. Turner, P. S., Thermal-expansion stresses in reinforced plastics, *J. Res. NBS*, **37**, 239-250, 1946.
98. Voigt, W., *Lehrbuch der Kristallphysik*, p. 962, Teubner, Leipzig, 1928.
99. Walpole, L. J., On bounds for the overall elastic moduli of inhomogeneous systems - I., *J. Mech. Phys. Solids*, **14**, 151-162, 1966a.
100. Walpole, L. J., On bounds for the overall elastic moduli of inhomogeneous systems - II., *J. Mech. Phys. Solids*, **14**, 289-301, 1966b.
101. Walpole, L. J., On the overall elastic moduli of composite materials, *J. Mech. Phys. Solids*, **17**, 235-251, 1969.
102. Walsh, J. B., New analysis of attenuation in partially melted rock, *J. Geophys. Res.*, **74**, 4333-4337, 1969.
103. Walsh, J. B., and W. F. Brace, The effect of pressure on porosity and the transport properties of rock, *J. Geophys. Res.*, **89**, 9425-9431, 1984.
104. Walsh, J. B., W. F. Brace, and A. W. England, Effect of porosity on compressibility of glass, *J. Am. Ceram. Soc.*, **48**, 605-608, 1965.
105. Wang, Z., and A. Nur, Ultrasonic velocities in pure hydrocarbons and mixtures, *J. Acoust. Soc. Am.*, **89**, 2725-2730, 1991.
106. Wang, Z., and A. Nur, *Seismic and Acoustic Velocities in Reservoir Rocks, Volume 2, Theoretical and Model Studies*, 457 pp., Society of Exploration Geophysicists, Tulsa, Oklahoma, 1992.
107. Watt, J. P., Elastic properties of polycrystalline minerals: Comparison of theory and experiment, *Phys. Chem. Minerals*, **15**, 579-587, 1988.
108. Watt, J. P., G. F. Davies, and R. J. O'Connell, Elastic properties of composite materials, *Rev. Geophys. Space Phys.*, **14**, 541-563, 1976.
109. Weissberg, H. L., and S. Prager, Viscous flow through porous media. III. Upper bounds on the permeability for a simple random geometry, *Phys. Fluids*, **13**, 2958-2965, 1970.
110. Willis, J. R., Variational and related methods for the overall properties of composites, in *Advances in Applied Mechanics*, Vol. 21, edited by C.-S. Yih, pp. 1-78, Academic Press, New York, 1981.
111. Wood, A. W., *A Textbook of Sound*, p. 360, Bell, London, 1955.
112. Wu, T. T., The effect of inclusion shape on the elastic moduli of a two-phase material, *Int. J. Solids Struct.*, **2**, 1-8, 1966.
113. Wyllie, M. R. J., A. R. Gregory, and L. W. Gardner, Elastic wave velocities in heterogeneous and porous media, *Geophysics*, **21**, 41-70, 1956.
114. Wyllie, M. R. J., A. R. Gregory, and G. H. F. Gardner, An experimental investigation of factors affecting elastic wave velocities in porous media, *Geophysics*, **23**, 459-493, 1958.
115. Zimmerman, R. W., Elastic moduli of a solid containing spherical inclusions, *Mech. Mater.*, **12**, 17-24, 1991.
116. Zimmerman, R. W., Hashin-Shtrikman bounds on the Poisson ratio of a composite material, *Mech. Res. Commun.*, **19**, 563-569, 1992.